

1
2
3
4
5
6
7
8
9
10
11
12
13
14
15
16
17
18

Life cycle comparison of industrial-scale lithium-ion battery recycling and mining supply chains

Michael L. Machala^{a,c,#}, Xi Chen^{b,#}, Samantha P. Bunke^{b,#}, Gregory Forbes^a, Akarys Yegizbay^d, Jacques de Chalendar^a, Inês L. Azevedo^{a,c}, Sally Benson^{a,c}, William A. Tarpeh^{b,c,*}

^a*Department of Energy Resources Engineering, Stanford University, Stanford, California, 94305, United States*

^b*Department of Chemical Engineering, Stanford University, Stanford, California 94305, United States*

^c*Precourt Institute for Energy, Stanford University, Stanford, California 94305, United States*

^d*Department of Physics, Department of Economics, Kenyon College, Gambier, Ohio 43022, United States*

denotes equal co-first author contribution

** Corresponding author: email: wtarpeh@stanford.edu*

19 **Abstract**

20 Recycling lithium-ion batteries (LIBs) can supplement existing supplies of critical materials and
21 improve the environmental sustainability of LIB supply chains. In this work, environmental
22 impacts (greenhouse gas emissions, water consumption, energy consumption) of industrial-scale
23 production of battery-grade cathode materials from used LIBs are compared to the environmental
24 impacts of conventional mining supply chains. Refining mixed-stream LIBs into battery-grade
25 materials reduces these environmental impacts by at least 59%. Recycling batteries to mixed metal
26 products instead of discrete salts further reduces environmental impacts. Electricity consumption
27 is identified as the principal contributor to all LIB recycling environmental impacts, and different
28 electricity sources can change greenhouse gas emissions up to eight times. Supply chain steps that
29 precede refinement (material extraction and transport) contribute marginally to the environmental
30 impacts of circular LIB supply chains (<5%), but are more significant in conventional supply
31 chains (31%). This analysis disaggregates conventional and circular steps based on material
32 extraction, transport, and industrial refinement operations; provides important insights for
33 advancing sustainable LIB supply chains; and informs optimization of industrial-scale
34 environmental impacts for emerging battery recycling efforts.

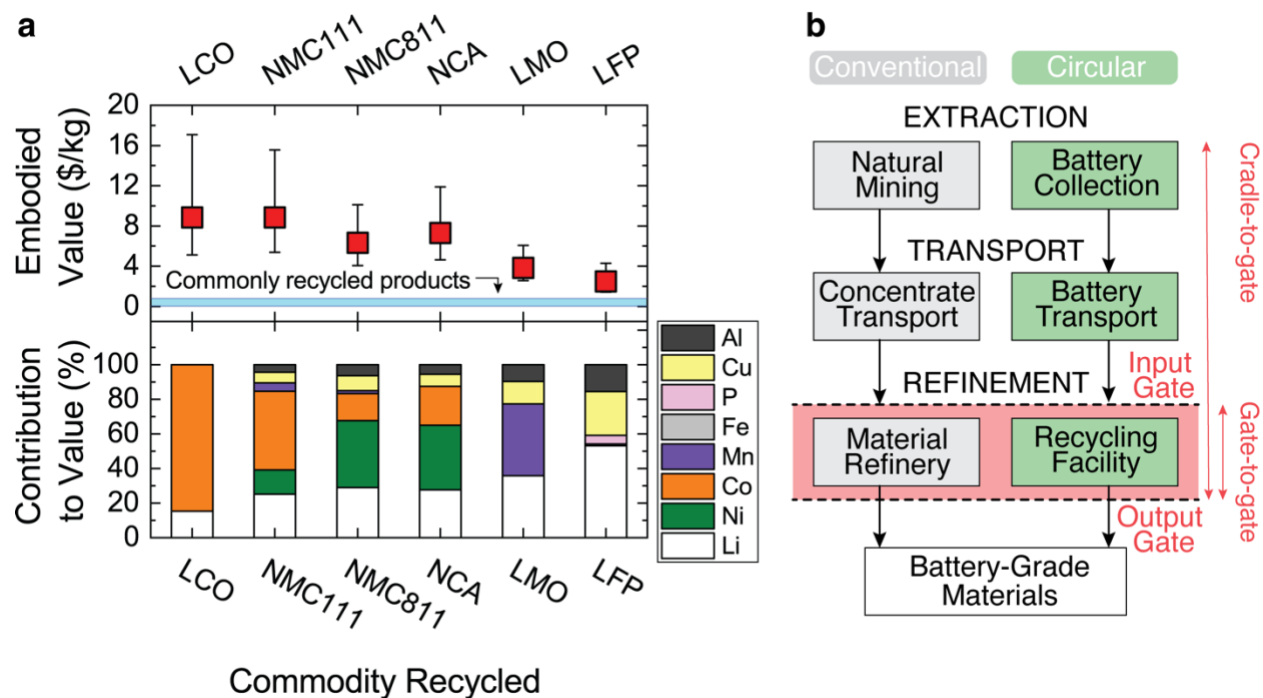
35

36 **Keywords:** circular economy, critical materials, hydrometallurgy, life cycle assessment,
37 pyrometallurgy, reductive calcination

38 The rise of intermittent renewable energy generation and vehicle electrification has created
39 exponential growth in lithium-ion battery (LIB) production beyond consumer electronics. By
40 2030, the electric vehicle (EV) sector is projected to dominate LIB growth, accounting for 82% of
41 an estimated 2.4 TWh yr⁻¹ of total global LIB production (**Fig. S1, Supplementary Information**).
42 However, the limited supply of critical materials (e.g., Li, Ni, Co, and Cu¹) needed for prominent
43 LIB chemistries has exacerbated environmental, economic, national security, and human rights
44 concerns^{2,3}. Critical LIB materials are projected to reach major global supply-demand balance
45 deficits before 2030 (**Fig. S1**). Further, both mining of LIB materials and improper disposal of
46 end-of-life LIBs can damage natural and human ecosystems, cause occupational hazards during
47 handling, and result in monetary losses⁴.

48 Recycling critical materials in end-of-life LIBs can help alleviate growing environmental
49 concerns and is essential for the long-term sustainability of electrified transportation. While
50 recycled materials may not contribute substantially to global LIB demand for decades, the
51 establishment of domestic circular supply chains is iterative, requiring multiple learning curves as
52 the dominant supply of end-of-life LIB chemistries and form factors evolve and as supply grows.
53 Factors central to the success of recycling include the ease of collecting products, the cost of
54 recycling processes, and the economic value of recovered materials. The average embodied
55 economic values of representative LIBs between 2018–2021 are shown in **Fig. 1a** (complete
56 references are listed in **Supplementary Information**). In LIBs, between 2018–2021, Li, Ni, and
57 Co comprise the highest embodied economic value, and Al and Cu account for a significant weight
58 percentage of EV battery packs (approximately 25%)⁵. Despite an embodied economic value that
59 is 2–10 times higher compared to the lead in lead-acid batteries, LIBs are only recycled 2–47%
60 globally⁶, compared to 99% for lead-acid batteries in the U.S. Regardless, the untapped potential
61 of LIB recycling constitutes a significant economic and environmental opportunity that requires
62 evaluation across several application scales, from numerous small-scale consumer electronic LIBs
63 (e.g., 10–100 Wh) to fewer large-scale transportation and stationary storage LIB packs (e.g., 10–
64 100 kWh)⁷. In addition, the preferred chemistries by automakers have evolved to hedge potential
65 critical mineral shortages and react to market shifts, such as the near tripling of lithium carbonate
66 prices in early 2022. Existing LIB variation and supply chain complexity highlight the need for a
67 methodical and comparative life cycle assessment (LCA) between circular (i.e., recycling used

68 batteries) and conventional supply chains, which is also necessary for future recycling of the
 69 evolving portfolio of battery chemistries.



70
 71 **Fig. 1 | Economic drivers of lithium-ion battery (LIB) recycling and supply chain options for**
 72 **producing battery-grade materials. a**, Commodity values of representative LIBs (upper panel)
 73 and relative contributions of embodied metal elements to the LIB values (lower panel).
 74 Representative LIBs are from consumer electronics using lithium cobalt oxide (LCO), and electric
 75 vehicle battery packs including lithium nickel manganese cobalt oxide (NMC111 and NMC811),
 76 lithium nickel cobalt aluminum oxide (NCA), lithium manganese oxide (LMO), and lithium iron
 77 phosphate (LFP). Data are based on market values adjusted for inflation between January 2018
 78 and December 2021 (complete references are listed in **Fig. S1** in **Supplementary Information**),
 79 and the uncertainty denotes a 90% confidence interval, which may overlap with the data point in
 80 some instances, obscuring their view. The blue shaded area in the upper panel represents the
 81 average commodity values of commonly recycled products: glass, paper, plastic, and metal cans
 82 (more details are provided in **Fig. S1**). **b**, Cradle-to-gate steps of manufacturing battery-grade LIB
 83 materials (i.e., salts) from conventional and circular supply chains, both of which include three
 84 steps: extraction, transport, and refinement. Extraction and transport are considered upstream steps
 85 relative to gate-to-gate refinement, which is indicated by the red shaded area between “input” and
 86 “output” gates. Cradle-to-gate analysis considers the refinement and upstream processes together.

87
88 Despite significant progress, current understanding of the relative environmental impacts
89 of recycling LIBs is still incomplete. The most significant environmental differences between LIB
90 production from circular and conventionally mined cathode material lie early in supply chains,
91 comprised of extraction, transport, and refinement steps (together “cradle-to-gate,” **Fig. 1b**). While
92 several previous studies have investigated cradle-to-gate environmental impacts, gate-to-gate
93 analyses of circular refinement processes are inconsistent, reporting environmental impacts that
94 differ by >30%⁸⁻¹⁰, and are not completely based on industrial-scale LIB recycling operations. The
95 gate-to-gate refinement processes utilized at established and emerging circular refinement
96 facilities may include mechanical separation (Me), pyrometallurgy (Py), and hydrometallurgy
97 (Hy)^{8,9}. Specifically, Me physically dismantles LIBs into constituent components, Py leverages
98 elevated temperature to facilitate thermally-driven material transformations, and Hy separates
99 materials in the aqueous phase via leaching, precipitation, and solvent extraction processes.
100 Variations in environmental impacts arise from the specific operational choices at refinement
101 facilities that utilize different processing pathways and from the methods to evaluate them. There
102 is a critical need for transparency and detailed insights into the environmental impacts (e.g., energy
103 consumption, greenhouse gas emission, and water consumption) of LIB refinement pathways and
104 all cradle-to-gate supply chain steps. Previous efforts have worked towards addressing this
105 need^{8,11}, and this study builds on the comparative methodology of a recent step-by-step study to
106 provide higher resolution and more actionable primary data, insights, and recommendations.
107 Advancing decision-making capabilities to scale sustainable LIB supply chains requires life cycle
108 assessment with more granular data at each step, inclusion of industrial-scale refinement
109 operations with practical mixed-stream battery feedstocks, documentation of operational
110 parameters, and qualification of results in terms of limitations and applicability to real-world
111 scenarios.

112 In this study we quantify the cradle-to-gate environmental impacts of battery-grade cathode
113 material salts manufactured in conventional and circular supply chains across three major steps:
114 material extraction, transport, and refinement (**Fig. 1b**). First, we quantify and compare the
115 refinement of mined concentrate from natural deposits into battery-grade materials in conventional
116 supply chains with production of these materials by Redwood Materials (a recycling company in
117 Nevada, U.S.). Two LIB feedstocks are explored: non-energized LIB production scrap from

118 manufacturing facilities and energized end-of-life LIBs collected from consumers. Industrial-scale
119 operational data provided by Redwood Materials are analyzed and compared to conventional LIB
120 supply chain values based on Argonne National Laboratory's Greenhouse Gases, Regulated
121 Emissions, and Energy use in Technologies (GREET 2021) model¹². Second, influences of the
122 product formats in the refinement pathways on environmental impacts are examined. For both
123 conventional and circular refinement, impacts of producing mixed Ni-Co compounds and discrete
124 salts are analyzed. Third, we assess the environmental impacts of upstream processes before gate-
125 to-gate refinement based on modeling. The upstream assessment includes the extraction of LIB
126 material from conventional (i.e., mined ore) or circular (i.e., collected batteries) sources and the
127 transport of extracted material to relevant refinement facilities for production of battery-grade
128 cathode materials as Li, Co and Ni sulfate or carbonate salts. To the best of our knowledge, this
129 study is the first life cycle assessment with primary industrial-scale circular refinement data that
130 includes stepwise, cradle-to-gate comparison of conventional and circular LIB supply chains. With
131 the methodologies and results reported herein, researchers can prioritize major opportunities to
132 improve process efficiencies, practitioners can benchmark their environmental impacts, and
133 policymakers can incentivize best environmental practices in LIB supply chain management.
134 Insights provided by this study can also help recyclers optimize the environmental impacts of their
135 refinement processes.

136 **Results**

137 In LIB supply chains, the refinement step converts the collected feedstocks into battery-grade salts
138 for further manufacturing (**Fig. 2a**). In both conventional and circular supply chains, the
139 refinement pathways vary significantly depending on multiple factors. Five refinement pathways
140 are compared in this study (**Fig. 2b**). While conventional refinement starts with mined ores/brines
141 (1 and 2), circular refinement starts with either end-of-life batteries (1 and 2) or battery scrap (5).
142 Ni and Co in refinement products for subsequent manufacturing can be discrete salts (1 and 3) or
143 mixed compounds (2, 4, and 5).

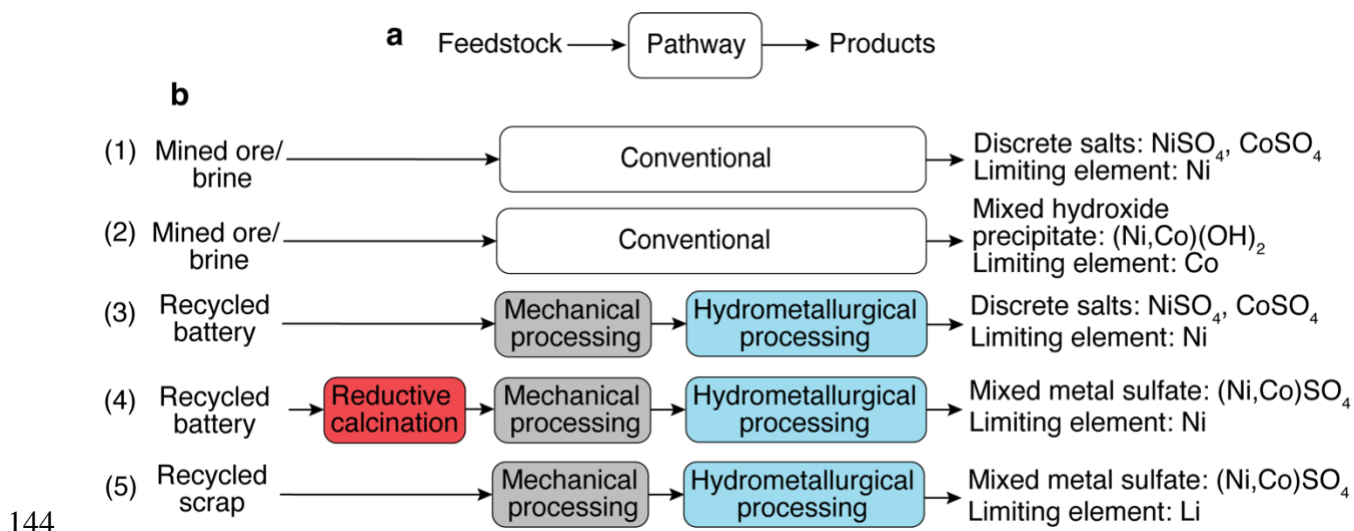
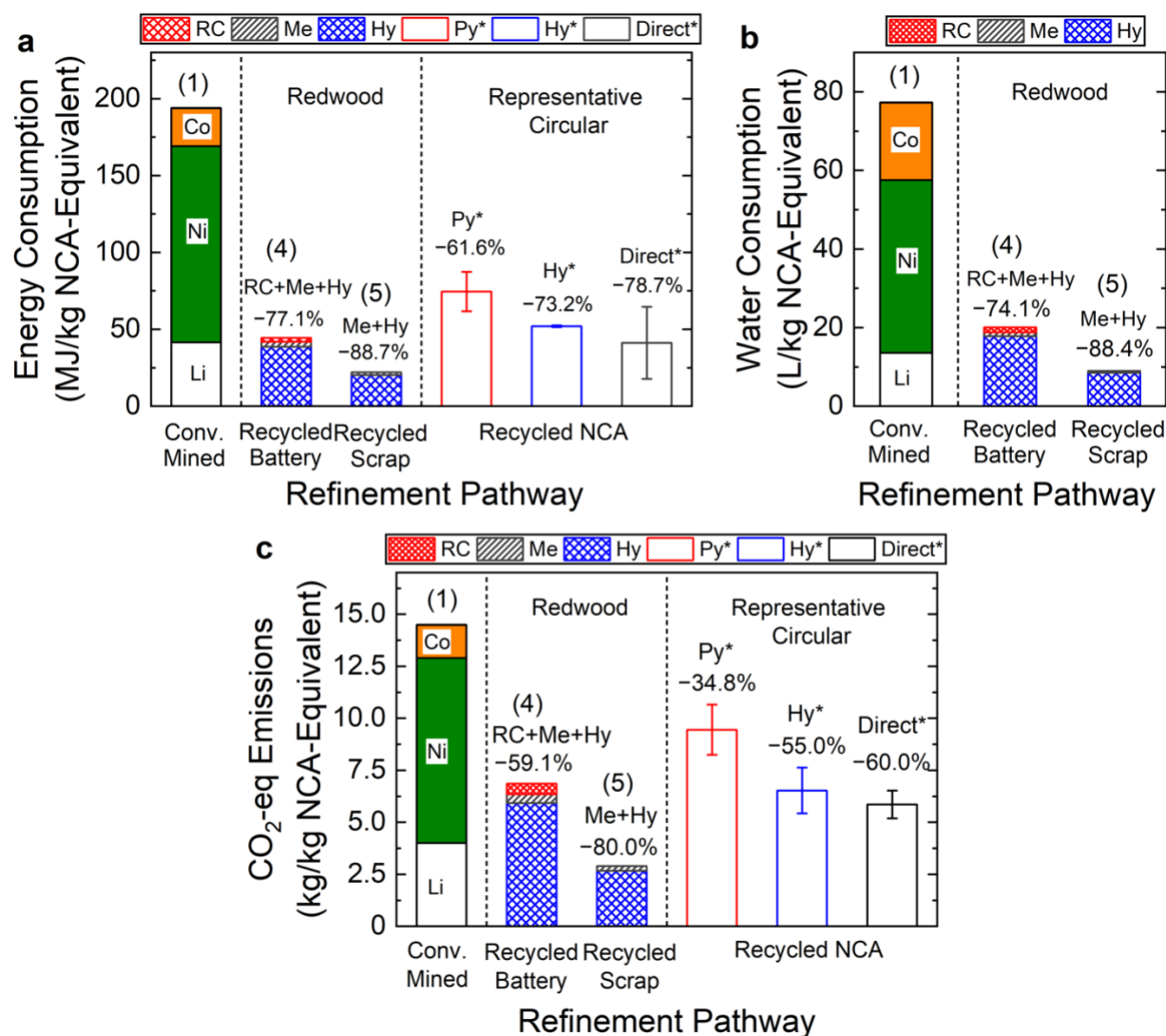


Fig. 2 | Schematic summarizing feedstocks, pathways, and products in refinement analyses.
a, General schematic showing the feedstock, pathway, and products as a legend for the refinement methods shown below. **b**, Five specific refinement analyses in this study: conventional refining (1 and 2) receives mined ore and brines, and circular refining methods (3–5) recycle from end-of-life batteries or scraps. While all methods produce identical Li₂SO₄ and Al₂O₃, Ni and Co products exist in the form of discrete salts, NiSO₄ and CoSO₄ (1 and 3), mixed hydroxide (Ni,Co)(OH)₂ (2), or mixed metal sulfate (Ni,Co)SO₄ (4–5).

Refining lithium-ion batteries into battery-grade materials exhibits lower environmental impacts than production from mined natural materials. The upstream steps of material extraction and transport are considered in later sections. Environmental impacts including energy consumption, greenhouse gas emissions (CO₂-equivalents, CO₂-eq; additional criteria air pollutants are detailed in **Table S1**) and water consumption of refinement pathways in conventional and circular LIB supply chains are compared in **Fig. 3** for the gate-to-gate production of battery-grade cathode materials. State-of-the-art conventional pathways generating discrete salts (Method (1) in **Fig. 2**) are analyzed here. One kg of lithium-nickel-cobalt-aluminum-oxide cathode-equivalent material (NCA-eq) is employed as a functional unit throughout this study for supply chain comparison, accounting for the elemental requirements to produce stoichiometric LiNi_{0.80}Co_{0.15}Al_{0.05}O₂. NCA chemistry is selected for the functional unit because it comprises the second-largest category of EV battery chemistries following NMC batteries^{7,13}, and is projected to utilize less Co compared to NMC⁶. Excluding the environmental impacts of material extraction

166 and transport steps, the gate-to-gate production of one kg NCA-eq battery-grade material from
 167 conventional mined natural materials consumes 193.9 MJ and 77.3 L H₂O while emitting 14.5 kg
 168 CO₂-eq (**Fig. 3**). The values of energy consumption and greenhouse gas emissions are comparable
 169 with previous studies based on GREET datasets^{11,12} (**Fig. S3**). Refinement of mined material
 170 concentrate into battery-grade Ni material dominates NCA environmental impacts,
 171 representing >57% of total values.



172
 173 **Fig. 3 | Environmental impacts of conventional and circular refining technologies.** a, Energy
 174 consumption, b, CO₂-eq emissions, and c, water consumption of gate-to-gate refinement by
 175 different pathways for NCA battery-grade salts. Numbers in parentheses labelled on the top of
 176 stacked bars denote the refinement methods summarized in **Fig. 2**. The conventional mined

177 pathway (Conv. Mined) refines natural deposits and produce discrete salts (Method (1) in **Fig. 2**);
178 note that Al is presented on the top of the stacked bars but its contributions are too small to be seen;
179 however specific environmental impacts of each element contributor are detailed in Table S1.
180 Circular supply chains refine from either mixed energized end-of-life lithium-ion batteries
181 collected from consumers (Recycled Battery, Method (4) in **Fig. 2**) or non-energized battery scrap
182 from a production facility (Recycled Scrap, Method (5) in **Fig. 2**), producing mixed metal sulfates.
183 Multi-step circular refinement pathways include mechanical processing (Me, grey), reductive
184 calcination (RC, red), and hydrometallurgy (Hy, blue). RC is an additional processing step for
185 energized batteries and is not used for non-energized recycled scrap. Open bars in the right panels
186 denote environmental impacts of recycling NCA batteries with representative existing
187 pyrometallurgical (Py*), hydrometallurgical (Hy*), and direct recycling (Direct*) methods as
188 comparison, and data are obtained from the literature⁸. Literature data is normalized by the same
189 functional unit in this study, and uncertainties are determined by combining two different battery
190 form factors: pouch and cylindrical (detailed in **Table S14–S15**). The vertical dashed line in each
191 graph demarcates different data types, where the model-based conventional and representative
192 existing pathways are summarized in the left panel, operational data from Redwood Materials are
193 presented in the middle panel, and literature data in the right panel. Note that water consumption
194 has generally not been quantified in previous studies, leading to no literature data panel for **Fig.**
195 **3b**. Environmental impacts of material extraction and transport in the supply chains are not
196 included.

197

198 The environmental impacts of two circular refinement pathways are presented in each
199 graph in **Fig. 3** for mixed-stream LIB feedstocks processed at Redwood Materials: non-energized
200 production scrap from LIB production facilities (recycled scrap) and energized, end-of-life LIBs
201 collected from consumers (recycled battery). Using a limiting-reagent approach of output products
202 to produce one kg NCA-eq material, energy requirements for processing recycled scrap and
203 recycled battery streams are 22.0 MJ/kg and 44.4 MJ/kg NCA-eq materials, significantly lower
204 than conventional refinement by 88.7% and 77.1%, respectively (**Fig. 3a**). Relatedly, 2.9 and 6.9
205 kg CO₂-eq/kg NCA-eq materials are generated from scrap and battery streams, respectively, a
206 substantial reduction in CO₂-eq emissions by 80.0% and 59.1% (**Fig. 3b**). Water consumption is
207 also lower by 88.4% for scrap and 74.1% for battery streams relative to the conventional scenario,

208 resulting from the consumption of 9.0 and 20.0 L H₂O/kg NCA-eq materials, respectively (**Fig.**
209 **3c**). Note that while the elemental stoichiometry is identical, the output battery-grade materials
210 vary slightly between conventional (Li₂CO₃, NiSO₄, CoSO₄) and circular (Li₂SO₄, (Ni, Co)SO₄)
211 supply chains (detailed in **Methods**). Converting the final lithium product to Li₂CO₃ does not
212 substantially change the environmental impacts of the circular supply chains (Supplementary Note
213 3, **Fig. S3**), and impacts of producing discrete or mixed products are examined in the following
214 section.

215 To produce battery-grade cathode materials, Redwood Materials uses a combination of
216 reductive calcination (RC), mechanical (Me), and hydrometallurgical (Hy) LIB refinement
217 processes (pathways detailed in **Fig. S2**). The RC process converts energized battery feedstock
218 under certain conditions that leverage heat from exothermic processes and inhibit graphite
219 combustion. This process does not use direct fossil fuel inputs onsite and facilitates subsequent
220 hydrometallurgical refinement into battery-grade materials. Because RC is not required for non-
221 energized LIB production scrap materials, the two feedstock streams (recycled scrap and recycled
222 batteries) are analyzed separately. Energy consumption and CO₂-eq emissions of representative
223 existing recycling pathways from the literature, including pyrometallurgy (Py*), hydrometallurgy
224 (Hy*), and direct recycling (Direct*), are also presented in **Fig. 3** for comparison. In general, the
225 RC+Me+Hy pathway at Redwood exhibits comparable energy consumption and CO₂-eq emissions
226 with Hy and Direct literature values⁸, and substantially lower environmental impacts than Py*.
227 Note that traditional pyrometallurgy and Redwood Material's reductive calcination can process
228 energized batteries of varying states of charge, health, and formats with minimal modification,
229 whereas traditional hydrometallurgy may need to discharge energized batteries in salt bath or
230 cryogenically remove electrolyte for safe mechanical processing. While this analysis is focused on
231 Redwood Materials refinement pathways, the methodology can be used to evaluate additional
232 refinement pathways (e.g., hydrometallurgy in **Fig. S3c**), or others that use different material
233 feedstocks, refinement processes, and energy supplies.

234 Among the few studies that directly compare environmental impacts of circular and
235 conventional NCA refinement using industrial-scale operational data, 35% lower greenhouse gas
236 emissions (**Fig. S3**) are reported for Me+Hy circular refinement compared with the current
237 study^{8,11}. However, direct comparison can be inexact due to varying underlying assumptions and
238 data sources. For example, Argonne National Laboratory's GREET and EverBatt models leverage

239 a combination of technology descriptions from patent applications (the most recent from 2007),
240 literature data on process flow consumptions, industry site visits and surveys, expert advice
241 solicitation, and stated assumptions to form complete pathways. Further, Ciez and Whitacre
242 quantified environmental impacts using output products represented as “metal offsets” for
243 pyrometallurgy or with metals in solution for hydrometallurgy⁸ (**Note 3 in Supplementary**
244 **Information**), rather than cathode salts in this study. In addition, the previous studies included a
245 portion of recycled metal materials in its conventional supply chain analysis, whereas this work
246 references only mined natural deposits in conventional supply chains to fully deconvolute the
247 environmental impacts¹¹. The different conclusions highlight divergent life cycle assessment
248 approaches, processing conditions, and the utility of primary industrial data access over modeling
249 processes from literature sources.

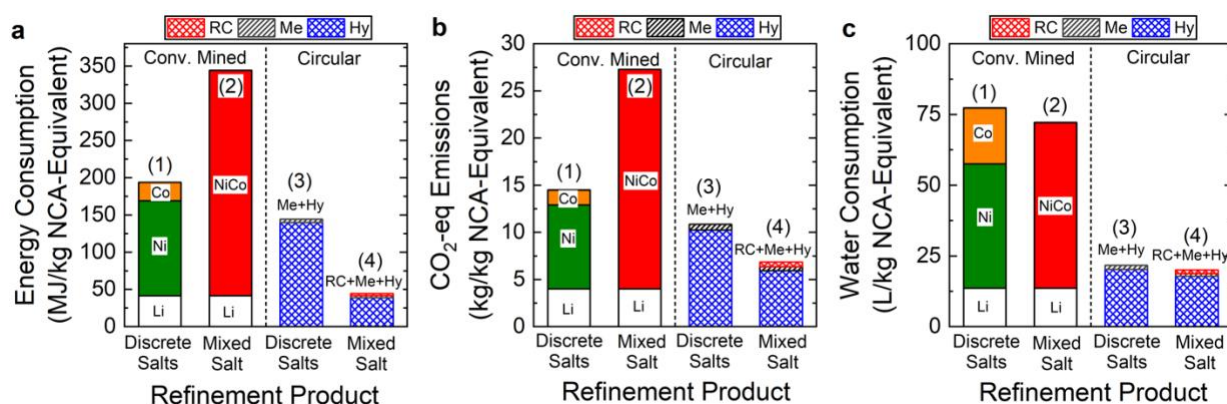
250 **Formats of refinement products influence environmental impacts**

251 Ni and Co are key elements for battery manufacturing, and can be traded in the format of mixed
252 metal salts or discrete salt products between battery refiners and battery manufacturers^{14,15}. To
253 examine the influences of the refinement product formats, the environmental impacts of refinement
254 to mixed salt are compared to the refinement to discrete sulfate salts, NiSO₄ and CoSO₄ (**Fig. 4**).
255 Both conventional and circular refinement pathways are analyzed.

256 The GREET model is employed to analyze different conventional mining pathways
257 generating different product formats (detailed in **Methods**). In conventional mining, refining Ni-
258 Co ores to mixed hydroxide precipitate, (Ni,Co)(OH)₂ (Method (2) in **Fig. 2**), elevates energy
259 consumption and CO₂-eq emissions by 77.% and 89.4%, respectively, over the discrete salts-based
260 pathway (**Fig. 4A** and **4B**, left panels). While the discrete products NiSO₄ and CoSO₄ are produced
261 from the mixed hydroxide precipitates through additional post-treatment, the very low composition
262 of Co (3.6%) in the latter limits the NCA stoichiometry, thus increasing the total energy cost to
263 generate 1 kg NCA-equivalent materials. On the other hand, water consumption of refining mixed
264 hydroxides is slightly lower (−6.6%) than that in producing discrete salts.

265 Circular pathways refining batteries to different products are analyzed using the Redwood
266 data by the RC+Me+Hy process and the modeling of a representative battery recycling method
267 combining mechanical and hydrometallurgy (Me+Hy) refinement (Method (3) in **Fig. 2**). The
268 Redwood process refines recycled batteries to mixed metal sulfate, (Ni,Co)SO₄, whereas the

269 representative Me+Hy produces discrete NiSO₄ and CoSO₄ as the products. The RC pathway
 270 (RC+Me+Hy) exhibits lower energy consumption (−72.3%), CO₂-eq emissions (−39.5%), and
 271 water consumption (−12%) relative to the Me+Hy pathway (**Fig. 4**), because it avoids additional
 272 treatment separating (Ni,Co)SO₄ to discrete salts. Overall, our results indicate that refining
 273 batteries to mixed metal salts instead of discrete salts can substantially save environmental impacts
 274 while still satisfying the needs of circular LIB supply chains. Our findings also provide important
 275 insights to optimizing plant-scale battery refining operations. In the following sections, mixed salt-
 276 based pathways are analyzed for refinement.

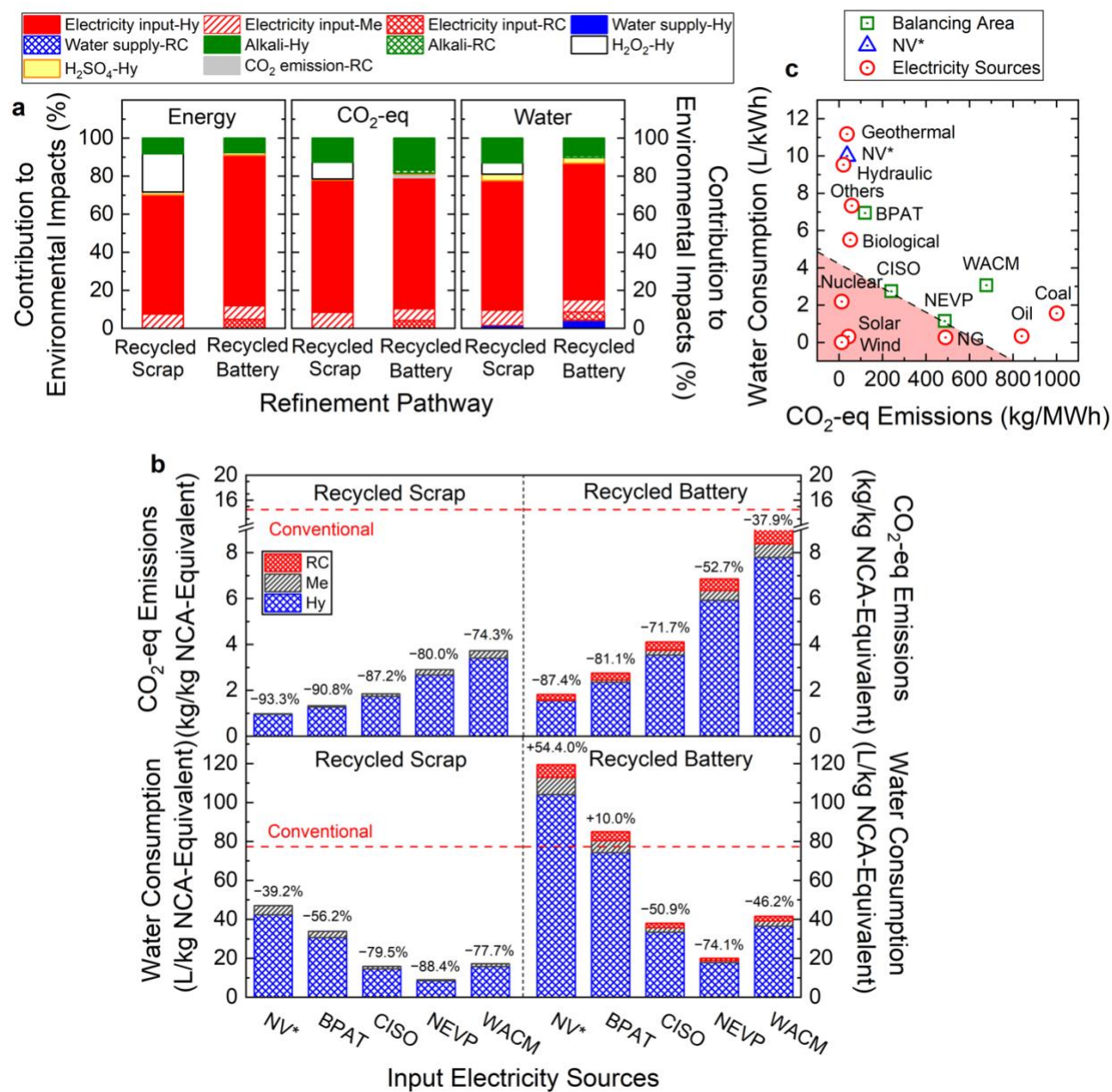


277
 278 **Fig. 4 | Influences of refining products on environmental impacts in circular refining. a,**
 279 **energy consumption, b, CO₂-eq emissions, and c, water consumption.** Left and right panels denote
 280 conventional (Conv. Mined) and circular pathways refining end-of-life batteries to discrete Ni and
 281 Co salts, or mixed Ni-Co salts. Note that Al is presented on the top of the stack bars of conventional
 282 supply chains but its contributions are too small to be seen (detailed values in **Table S1**). Numbers
 283 in parentheses labelled on the top of stacked bars denote the refining methods summarized in
 284 **Fig. 2**.

285
 286 **Electricity consumption dominates the environmental impacts of lithium-ion battery**
 287 **circular refinement.** The relative environmental impacts of input consumables (e.g., energy,
 288 water, commodity chemicals) in the gate-to-gate refinement processes are disaggregated in **Fig. 5**
 289 (additional criteria air pollutants in **Tables S2–S3, Figs. S4–S5**). Note that the embodied
 290 environmental impacts of electricity consumption in **Fig. 3** are based on the Nevada Power
 291 Company (NEVP) at the Redwood Materials location. Electricity consumption is a principal factor

292 dominating the environmental impacts. For both LIB feedstock pathways (Methods (4) and (5) in
293 **Fig. 2**), electricity accounts for 70.3–91.0% of the total energy consumption, 71.8–79.1% of the
294 total CO₂-eq emissions, and 54.3–63.6% of water consumption (**Fig. 5a**). For both feedstocks, Hy
295 processes comprise the majority of environmental impacts, contributing more than 87.3% to
296 energy consumption, 86.3% to CO₂-eq emission, and 88.8% to water consumption. Notably, the
297 additional RC step required for processing energized batteries only marginally contributes to CO₂-
298 eq emissions (7.4% of total). Unlike conventional pyrometallurgical processes that require external
299 energy sources^{8,16}, the RC process is primarily autothermic because it leverages process heat
300 released from exothermic reactions of the LIB materials^{17,18}. In addition to electricity consumption,
301 chemical reagents used in circular refinement processes also contribute to embodied environmental
302 impacts. Alkali reagents used to precipitate metals contribute between 19.0–21.3% of
303 environmental impacts (largest relative contribution to water consumption). H₂O₂ is used to reduce
304 high-oxidation state metal compounds for hydrometallurgical leaching of scrap material, and
305 accounts for 11.3–20.1% of environmental impacts (largest relative contribution to energy
306 consumption).

307



308

309 **Fig. 5 | Breakdown of environmental impacts of lithium-ion battery (LIB) recycling using**

310 **different input electricity sources.** a, Contributions to the environmental impacts of recycling

311 processes using electricity from the Nevada Power Company, including energy consumption, CO₂-

312 eq emission, and water consumption by different input consumables used in circular processes for

313 LIB feedstocks from production scrap (recycled scrap) and used energized batteries (recycled

314 battery) used by Redwood Materials. b, Environmental impacts of input electricity sources on

315 CO₂-eq emissions and water consumption in the LIB recycling operations employed by Redwood

316 Materials methods for production scrap and energized batteries. CO₂-eq emissions and water

317 consumption are based on the resources consumed by unit electricity generated from a Nevada
318 renewable energy tariff (NV*), Bonneville Power Administration (BPAT), California Independent
319 System Operator (CISO), Nevada Power Company (NEVP), and Western Area Power
320 Administration: Colorado-Missouri (WACM). The red dashed lines denote the environmental
321 impacts of the analogous conventional refining process. Note that influences of energy sources on
322 environmental impacts are only presented for the circular supply chains, but not for conventional
323 supply chains. Specific environmental impacts presented in the figures are detailed in **Table S5. c**,
324 Tradeoff relationship between embodied water consumption and CO₂-eq emission by different
325 power sources, including electricity grids in different locations (☉), purely power sources (☐),
326 and Nevada renewable energy tariff (NV*, △). The red dashed line denotes the lower bound of
327 the water-CO₂ performance, i.e., the existing electricity grids that have the lowest water
328 consumption and CO₂-eq emission simultaneously, and the green shaded area covers the power
329 sources that can transcend the current limit of water-CO₂ performance.

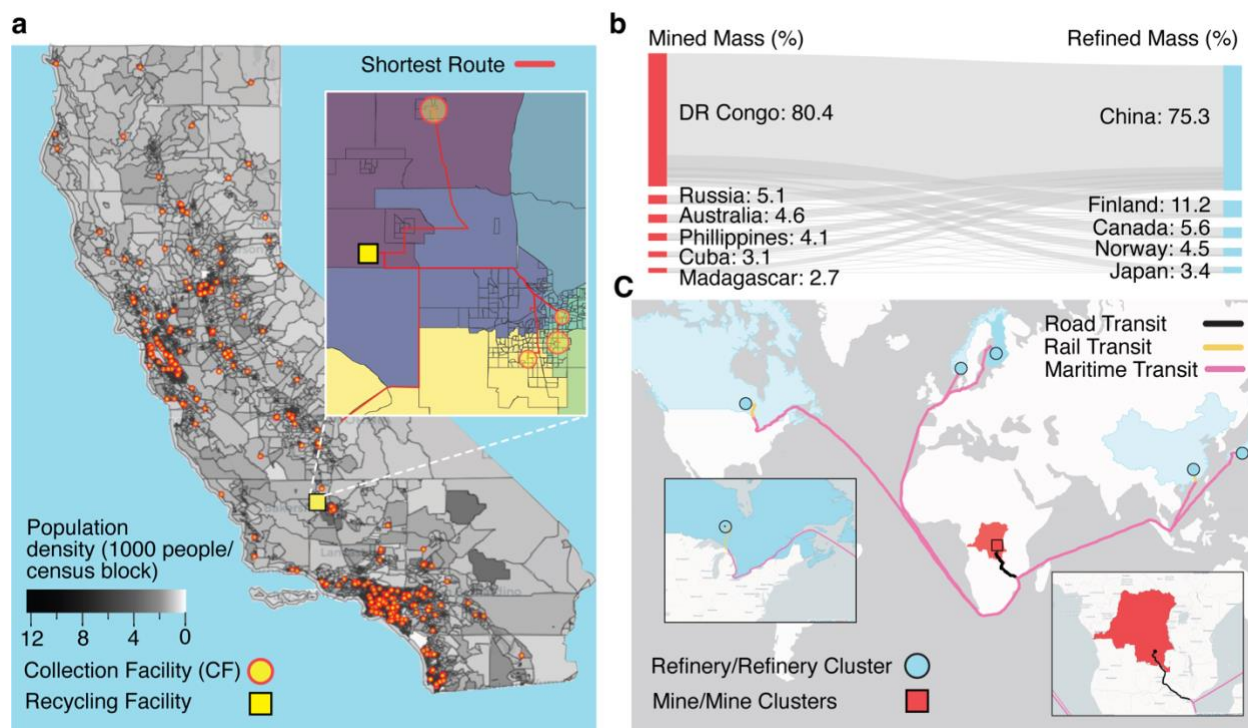
330

331 Because electricity dominates the environmental impacts of LIB recycling processes, a
332 comparison of electricity grid balancing areas that emit a range of CO₂-eq emissions per MWh
333 (averaged for 2019)¹⁹⁻²¹ are examined in **Fig. 5b** (additional criteria air pollutants detailed in **Table**
334 **S5**). Substituting NEVP electricity with other balancing areas including Bonneville Power
335 Administration Transmission (BPAT), California Independent System Operator (CISO), Western
336 Area Power Administration of Colorado-Missouri (WACM), and a 100% renewable energy tariff
337 in Nevada (NV*), yields a significant reduction in CO₂-eq emissions of up to 93.3% (recycled
338 scrap) and 87.4% (recycled battery) relative to conventional refinement (**Fig. 5b**). Conversely,
339 employing low-carbon electricity grids can increase water consumption compared with NEVP-
340 based operation, following the order of NV* > BPAT > WACM > CISO > NEVP (**Fig. 5b**). Note
341 that NV*- and BPAT-based circular refinement processes exceed the water consumption level of
342 conventional refinement due to significant contributions from hydro- and geothermal power.
343 Further investigation into the grid electricity sources of balancing areas reveals a tradeoff between
344 CO₂-eq emissions and water consumption based on electricity generation type (**Fig. 5c**); most
345 electricity sources with relatively low CO₂-eq emissions (e.g., those based on bio-, hydro-, or
346 geothermal energy) exhibit high water consumption, and vice versa. This tradeoff also explains
347 the different influences of electricity source on environmental impacts of the Redwood Materials

348 refinement step and other pathways (**Fig. S3d**). However, the electricity sources for each balancing
349 area will affect both CO₂-eq emissions and water consumption. For example, because NEVP-based
350 electricity includes a relatively large proportion (70%) from CO₂-eq emissions-intensive natural
351 gas with low water consumption, a switch to hydro-intensive (73%) BPAT electricity decreases
352 CO₂-eq emissions while increasing water consumption.

353

354 **Environmental impacts of material extraction and transport are significantly lower in**
355 **circular lithium-ion battery supply chains than in conventional supply chains.** Upstream of
356 gate-to-gate refinement are material extraction and transport to refinement facilities (**Fig. 1b**).
357 Environmental impacts of these upstream steps are analyzed for two representative LIB
358 chemistries and battery use cases: NCA in EV battery packs, and lithium cobalt oxide (LiCoO₂ or
359 LCO) in smartphones. California is chosen to assess circular extraction because it has the largest
360 population and EV market share of any state in the U.S.^{22,23}. Smartphones are considered extracted
361 when collected, aggregated, and transported from all California residents (analyzed per census
362 block) to the nearest existing collection facility (CF)²⁴. The analytical model for this circular
363 extraction is depicted in **Fig. 6a**, where a shortest-path route for collection from block group to CF
364 is modeled²². To quantify conventional material extraction environmental impacts from mining,
365 global supply chain data are adapted from GREET (**Table S6–S7**)¹². Smartphone extraction in the
366 circular supply chain emits only 0.0189 kg CO₂-eq/kg LCO-eq, significantly lower than
367 conventional mining (1.96 kg CO₂-eq/kg LCO-eq) by 99.0%. Energy and water consumption are
368 similarly lower in the circular supply chain (**Table S9**).



369

370 **Fig. 6 | A logistics model for assessing upstream environmental impacts of extraction and**

371 **transport in circular and conventional lithium-ion battery supply chains. a,** Modeled circular

372 extraction of LCO-based smartphones from every census-block group based on population to the

373 closest, existing private or municipal collection facility (CF) using a shortest-route algorithm. Inset

374 details modeled circular transport of smartphones aggregated at CFs and then transported to a

375 central recycling facility at the center (gravity point) of the California population by the shortest

376 route (red lines). Colors of block groups indicate the catchment area of a specific CF, where CF

377 size shows the relative number of smartphones collected in 2019. **b,** A weighted distribution

378 estimate of international transport logistics for conventional supply chains between mining and

379 refining countries based on cobalt productivity in the top Sankey diagram. **c,** An example of

380 transport logistics for cobalt mined and aggregated in the Democratic Republic of the Congo (DRC)

381 and then shipped via primary road, train rail, and maritime routes using a shortest-distance path to

382 major refinery locations, with insets showing the degree of detail considered. Similar analyses

383 were performed for Li, Ni, Co, and Al. Inserts present more detailed transit routes in DRC and

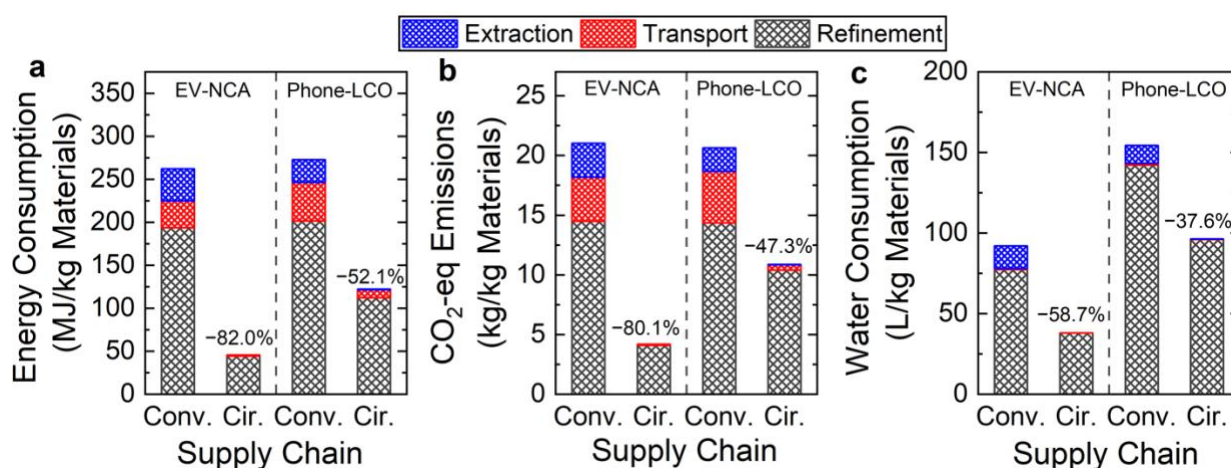
384 Canada.

385

386 After extraction, LIB material concentrates are transported along domestic and
387 international routes by truck, train rail, and maritime cargo ship to refinery locations (**Fig. S7** and
388 **Table S8–S15**; complete references in **Supplementary Information**). An algorithm is developed
389 to quantify environmental impacts based on a weighted distribution of participating countries and
390 the shortest distance along major transport routes (the case of cobalt is presented as an example in
391 **Fig. 6b**.) Conventional mine-to-refinery environmental impacts are calculated for one kg of
392 embodied Li, Ni, Co, and Al metal (**Table S7**). While transport emissions for Li, Ni, and Co range
393 from 5.4–6.4 kg CO₂-eq/kg embodied metal, Al is three times lower. For the circular case applied
394 to California, smartphones and EV battery packs collected at CFs are transported to a hypothetical
395 central LIB circular refinement facility at the population-weighted center (i.e., gravity point) of
396 California (near Bakersfield)²². In conventional supply chains, transporting mined material
397 concentrates accounts for 3.68 kg CO₂-eq/kg NCA-eq and 4.32 kg CO₂-eq/kg LCO-eq. By
398 comparison, emissions for the transport of aggregated end-of-life NCA EV battery packs (i.e., not
399 disassembled) and LCO smartphone batteries (not separated from phones) to a circular refinement
400 facility are 0.073 kg CO₂-eq/kg NCA-eq and 0.47 kg CO₂-eq/kg LCO-eq, 98.2% and 89.1% lower
401 than transport of mined concentrate, respectively. The reduction in CO₂-eq emissions is attributed
402 to differences in elemental concentrations of transported materials and aggregate transport distance
403 (e.g., a weighted average of 224 km for circular NCA-eq materials, and 57,600 km for conventional
404 NCA-eq materials).

405
406 **The refinement step dominates environmental impacts of circular and conventional supply**
407 **chains.** Combining material extraction, transport, and refinement steps yields a cradle-to-gate
408 comparison of the most differentiated steps of conventional and circular LIB supply chains for
409 producing battery-grade cathode materials (**Fig. 7**). Here the environmental impacts of the LIB
410 refinement step in California are analyzed for a hypothetical scenario employing the same circular
411 multi-step refinement technologies as Redwood Materials (i.e., RC+Me+Hy) in Nevada, but using
412 California (CISO) electricity to produce battery-grade cathode materials. A circular supply chain
413 in California for NCA EV and LCO smartphone batteries lowers energy and greenhouse gas
414 emissions by at least 47.3% and water consumption by over 37.6%. In the case of recycling NCA
415 EV batteries in California, the entire cradle-to-gate greenhouse gas emissions of the circular supply
416 chain are lower than the transport emissions of mined concentrate in conventional supply chains

417 (Fig. 7, Table S8). Circular production of LCO-grade materials leads to higher environmental
 418 impacts than that of NCA-grade materials based on the mixed-stream feedstock composition
 419 processed by Redwood Materials. Overall, upstream steps (extraction and transport) contribute
 420 marginally to the total environmental impacts of both circular supply chains, accounting for $\leq 4.9\%$
 421 CO₂-eq emission, $\leq 8.2\%$ energy consumption, and $\leq 0.24\%$ water consumption. Accordingly, the
 422 refinement process dominates the environmental impacts of the circular supply chain. In contrast,
 423 upstream steps in the conventional supply chain play a larger role (still smaller than refinement)
 424 in cradle-to-gate environmental impacts, contributing between 7.8–31.0% to the environmental
 425 metrics considered (Table S8).



426
 427 **Fig. 7 | Cradle-to-gate environmental impacts of different supply chains. a,** Energy
 428 consumption (left), **b,** CO₂-eq emissions (middle), and **c,** water consumption (right) of
 429 conventional (conv.) and circular (cir.) supply chains by step including material extraction,
 430 transport, and refinement. NCA-eq cathode used in electric vehicles (EV-NCA, left panels) and
 431 LCO-eq cathode material used in smartphones (Phone-LCO, right panels) are provided.
 432 Environmental impacts of refinement are analyzed based on electricity generated from balancing
 433 grid authority CISO and upstream supply chain steps (extraction and transport) are based on data
 434 from GREET and transport models developed in the preceding section and depicted in Fig. 6.
 435 Specific environmental impacts of each step are detailed in Tables S5–S7.

436 437 Discussion

438 This study is the first quantitative cradle-to-gate life cycle assessment of disaggregated
 439 conventional and circular LIB supply chains that include primary data from an industrial-scale

440 recycling facility. Practical LIB feedstock and refinement pathways are analyzed from recycling
441 company (Redwood Materials) and modeling is employed to examine the environmental impacts
442 of upstream material extraction and transport steps. The analysis reveals that refining end-of-life
443 LIBs into battery-grade cathode materials exhibits lower environmental impacts than conventional
444 refinement of mined materials, mixed salts products are more beneficial for circular refinement,
445 and the source of input electricity is the principal factor governing circular refinement
446 environmental impacts. Upstream circular supply chain steps contribute marginally to overall
447 environmental impacts, and the refinement step comprises the largest source of cradle-to-gate
448 environmental impacts.

449 Disaggregated analysis of LIB refinement pathways at Redwood Materials provides
450 important insights into the performance and potential of different refinement processes. While
451 pyrometallurgical processing is widely considered as more environmentally intensive than
452 hydrometallurgy, Redwood Materials' RC pathway exhibits much lower environmental impacts
453 than current Hy-containing pathways reported in practice and in literature (**Fig. S3**). The optimized
454 conditions of RC processing minimizes the combustion of carbon-containing LIB materials,
455 significantly reducing CO₂-eq emissions while simultaneously generating products that are
456 amenable for hydrometallurgical separation. Because chemical consumables such as H₂O₂ are
457 important contributors to hydrometallurgy, environmental impacts of Hy processes could be
458 reduced through more sustainable (e.g., electrochemical) production methods²⁵. Our findings also
459 advocate the refinement products of mixed metal sulfates over the single salts, indicating that the
460 further separations among Ni and Co salts can be avoided. An emerging alternative LIB recycling
461 technology, "direct recycling", recovers functional battery materials without decomposition into
462 substituent elements, and is reported to exhibit comparable environmental impacts to Redwood
463 Materials methods⁹. However, direct recycling is still under development and warrants further
464 assessment after process optimization and industrial-scale implementation.

465 Electricity greatly influences environmental impacts in LIB circular refinement, and the
466 variability among grid electricity sources elucidates a tradeoff between CO₂-eq emissions and
467 water consumption (**Fig. 5**). Therefore, considering water consumption and CO₂-eq emissions is
468 necessary for selecting recycling facility locations, particularly in water-sensitive or emissions-
469 sensitive scenarios. Further examination suggests that the tradeoff is primarily driven by water-
470 intensive hydroelectric and geothermal electricity in certain locations versus CO₂-intensive coal

471 and natural gas in others, implying that increasing the proportion of electricity from nuclear, wind,
472 and solar energy sources simultaneously reduces CO₂-eq emissions and water consumption
473 relative to existing balancing areas (**Fig. 5**).

474 Analyses of upstream environmental impacts inform better operations for future resource-
475 saving extraction and transport. Conventional mining and concentrating of ore or brine is resource-
476 intensive due to the low natural concentrations of critical materials (0.01–1%), while critical
477 material concentrations for transport rise to 3–15% after beneficiation. Further concentrating
478 materials near mine sites or building reinterests closer to sources can efficiently reduce
479 environmental impacts of the conventional mined materials. In contrast, smartphones contain 5%
480 LCO material by mass, with the batteries themselves at 24% LCO²⁵. Circular material extraction
481 via LIB collection decreases environmental impacts by 99% versus conventional. A “shortest-
482 route” approach is used in this study to quantify the environmental impacts of battery extraction
483 and transport supply chain steps. Practical battery collection operations will likely vary based on
484 route selection and preprocessing strategy further influencing environmental impacts²⁶. For
485 example, the disassembly of collected EV battery packs or removal of smartphone batteries from
486 devices prior to transport to a recycling facility can increase energy usage through extraction but
487 reduce environmental impacts by lowering transportation weight (**Table S10**). Trucks are used as
488 the primary vehicle for transport analysis given regulatory concerns that consider LIBs hazardous
489 material in many transportation scenarios²⁷. However, alternative transport like railway can further
490 lower environmental impacts by approximately four times versus trucking (**Tables S12**). Upstream
491 process optimization of environmental impacts warrants further investigation, such as the active
492 area of high-throughput automation of LIB extraction from non-standardized devices and EV
493 battery packs or rapid assessment of LIBS for second life uses.

494 While the current cradle-to-gate study is focused on Li, Ni, and Co as the major output
495 materials, the potential benefits of extracting additional LIB constitutive elements from ore (e.g.,
496 Cu and Co in Cu-Co sulfides) or from LIBs (e.g., Cu or Mn) warrants further investigation.
497 Additionally, the same mixed-stream LIB feedstocks consumed at Redwood Materials are used to
498 quantify NCA- and LCO-equivalent values, and results would vary for single-stream LIB
499 feedstocks. Generally, the incremental benefits of extracting additional critical materials from
500 concentrated sources like LIBs can offset the environmental impacts of both supply chains.

501 As the prevalence of LIBs grows in the mobility sector and beyond, strategic placement of
502 domestic LIB collection, refinement and manufacturing facilities can further minimize future
503 environmental impacts by considering heterogenous LIB growth by location, collection approach,
504 transportation distance, and electricity source for refinement processes. As LIB production scales,
505 policies informed by consumer surveys, focus groups, pilot testing, and diverse stakeholder
506 engagement will be needed to research and scale battery collection²⁸. Business models for
507 collection of all LIB types and sizes will likely vary from manufacturer-led to municipal or private
508 collection programs. In addition to collection costs, the varied scale of collection requires further
509 investigation, particularly for localized environmental impacts. Notably, analogous economic and
510 environmental impacts to local ecosystems of conventional mining are not considered in this
511 analysis, and warrant future studies²⁹. Additionally, designing and manufacturing LIBs for
512 recycling in a circular economy can reduce resource usage identified in this study³⁰. Future efforts
513 should also focus on optimizing refinement processes for subsequent steps of the circular supply
514 chain in LIB manufacturing, product performance, and economic cost.

515

516 **Methods**

517 **Goal and scope.** The goal of this study is to compare stepwise cradle-to-gate environmental
518 impacts (energy consumption, CO₂-eq emission, and water consumption) for two supply chains: a
519 conventional, linear supply chain fed by natural mined material for refinement into battery
520 materials, and a circular supply chain fed by LIBs. Both supply chains produce battery-grade
521 cathode materials. A cradle-to-gate analysis of the whole supply chain considers steps of material
522 extraction, transport, and refinement, and gate-to-gate analysis investigates the refinement step,
523 which is focused on in this study. A gate-to-gate scope is broadly defined as the boundary
524 surrounding processing facility operations. In this analysis, gate-to-gate refinement only considers
525 direct processing (e.g., alteration, concentration, precipitation) of the feedstock material once it is
526 extracted from its original state and transported to the refinement location (shown in **Fig. 1b**). For
527 Redwood Materials, this scope includes mechanical processing, reductive calcination, and
528 hydrometallurgy (**Fig. S2**). The system boundary does not include other operations outside of the
529 direct refinement processes as discussed in study limitations below.

530 Two LIB feedstock streams are evaluated: (1) battery production scrap and (2) mixed, spent
531 LIBs from consumers (**Fig. S2**). The study scope upstream of the gate-to-gate supply chain step
532 completes cradle-to-gate analysis, and includes both material extraction and transport steps. For
533 conventional extraction, GREET is used for quantifying the environmental impacts of mining.
534 Transport between supply chain steps and for the circular extraction step are quantified using a
535 logistics transportation model developed in this study, where limitations are summarized below.

536 **Methodology.** An attributional life cycle assessment is conducted to quantify and compare
537 conventional and circular LIB supply chains for the production of battery cathode materials. This
538 analysis complies with the International Organization for Standardization (ISO) 14040 standards
539 but omits conversion to environmental impact indicators and external review³¹. Data for
540 conventional material extraction (e.g., mining) and refining are adapted from the Argonne National
541 Laboratory's Greenhouse gases, Regulated Emissions, and Energy use in Transportation
542 (GREET®) 2021 model. GREET and the ecoinvent 3.3 database³² are employed for life cycle
543 inventory data of chemical consumables for the conventional and circular supply chains.

544 To assess circular LIB refinement, primary operational data detailing energy, water, on-
545 site emissions, and consumables usage are provided by Redwood Materials and normalized to
546 mass flows of the different elements of interest in input feedstocks and output products. A
547 representative prevailing circular refinement, Method (2) in **Fig. 2**, is modeled with the software
548 HSC Sim³³, based on the technical procedures available in the literature³⁴⁻³⁷ and the practical
549 feedstock amount received by Redwood.

550 Conventional refinement was modeled by aggregating the environmental impacts of the
551 individual refining pathways for each LIB cathode element (**Table S1**), normalizing by the mass
552 of the individual element of interest within the output product (e.g., Li in Li₂CO₃) and then
553 normalizing again by the mass of that element in the functional unit for this life cycle assessment
554 (defined in the next section). For elements where more than one pathway of production exists in
555 the GREET model (i.e., Ni and Li), the overall environmental impacts are calculated by averaging
556 pathways weighted by their respective share of global production (45% Li production from brine
557 and 55% from ore, and 60% Ni production from mixed hydroxide precipitate and 40% from Class
558 1 Ni). Both discrete and mixed output products are considered. Discrete salts from conventional
559 refinement are Li₂CO₃, NiSO₄, CoSO₄, and Al₂O₃; alternatively, (Ni,Co)(OH)₂ is considered as

560 the mixed product. Lithium outputs produced by Redwood Materials are Li_2SO_4 (environmental
561 impacts for converting to Li_2CO_3 are detailed in Supplemental Information **Note 3**), and other
562 outputs exist as mixed metal sulfates of $(\text{Ni}, \text{Co})\text{SO}_4$ or as Al_2O_3 and $\text{Al}(\text{OH})_3$. With additional
563 treatment further transform the mixed metal sulfate into separate Ni and Co compounds, discrete
564 salts as NiSO_4 and CoSO_4 are analyzed based on modeling of a prevailing Hy+Me refinement
565 pathway. In the cradle-to-gate analysis, material transportation between stages was not included
566 because it was not consistently available in the GREET model. Mixes vary between elements, as
567 well as between pathway stages. For example, crude production of $\text{Co}(\text{OH})_2$ uses a distributed
568 electricity source in the Democratic Republic of the Congo, and the refinement of these materials
569 into CoSO_4 and CoCl_2 uses a distributed electricity source in China. While exploring the sensitivity
570 of environmental impacts for conventional battery material production is important, it is beyond
571 the scope of this paper, and instead, this work focuses on the sensitivity of electricity sources in
572 U.S.-based LIB recycling. See **Supplementary Data File A** for the breakdown of the conventional
573 refining data workflow.

574 **Defining functional units.** Functional units standardize comparisons of the resource consumption
575 and emissions in life cycle assessments. In this study, two functional units are considered in this
576 assessment to normalize environmental impacts between conventional and circular supply chains:
577 the battery-grade material required to make one kg of stoichiometric lithium nickel cobalt
578 aluminum oxide ($\text{LiNi}_{0.80}\text{Co}_{0.15}\text{Al}_{0.05}\text{O}_2$, NCA-eq) and lithium cobalt oxide (LiCoO_2 , LCO-eq)
579 cathode material. Mass was selected as the primary normalizing factor because any energy-based
580 functional unit (e.g., per kWh) could vary based on battery manufacturing and cycling
581 characteristics. The NCA chemistry was selected because reports suggest future cathodes may
582 utilize less Co compared to NMC batteries in EVs, and NCA comprised the second-largest
583 category of EV battery chemistries in 2016, following NMC batteries⁷. LCO is a representative
584 chemistry used in handheld rechargeable devices (e.g., cellphones and laptops) which are currently
585 available to recycle in larger quantities than EV LIBs. The environmental impacts of other LIB-
586 relevant materials (Cu and Mn) in conventional supply chains can be found in **Table S7**.

587 In both conventional and circular supply chains, the extraction, transport, and refinement
588 steps are converted into environmental impacts metrics for the production of battery-grade
589 materials and normalized by NCA and LCO functional units. A limiting reagent approach is used

590 to quantify the environmental impacts of a functional unit in circular refinement pathways.
591 According to current multi-step pathways using mixed-stream LIB feedstocks (either recycled
592 scrap or recycled battery), the Li output is the limiting element for creating one kg of NCA-eq
593 materials from recycled scrap, where other refined elemental products are produced in excess.
594 Relatedly, Ni is the limiting output element from recycled batteries. For multi-step refinement
595 processes, the recovery rate of Ni and Co is 95% and for Li is 92%. Additionally, a sensitivity
596 analysis of environmental impacts from circular refinement is conducted based on facility location
597 in different grid balancing areas and their associated electricity sources.

598 **Life cycle inventory and assessment.** The life cycle inventory (LCI) data for conventional mining
599 pathways are normalized by each critical metal element: Li, Ni, Co, Al, Cu, and Mn (**Table S7**).
600 The LCI for consumables in the Redwood process are adapted from the GREET 2021 model and
601 ecoinvent 3.3 (**Table S2**).^{12,32} The LCI for the Redwood processes also lists water consumption
602 and criteria emissions for different electricity sources by grid balancing areas in the Western U.S.
603 (**Table S6**). Three categories of environmental impacts are detailed in this study: energy
604 consumption, air pollutant emissions, and water consumption. Energy consumption includes the
605 input electricity for different applications and the energy required to produce required
606 consumables. Criteria air pollutant emissions include the embodied emissions generated by the
607 production of input electricity and the consumed reagents. CO₂, CH₄, CO, NO_x, N₂O, SO_x, PM₁₀,
608 and PM_{2.5} are the air pollutants provided in the GREET model and considered here. The
609 greenhouse gas emissions are reported as CO₂ equivalents (CO₂-eq) summing CO₂, CH₄, and N₂O
610 weighed by the corresponding 100-year global warming potential (GWP). Water consumption
611 considers the withdrawn water that is not returned to the original source, and both the input city
612 water usage and the embodied water consumption in electricity generation and the manufacturing
613 of consumable materials are included.

614 **Estimating environmental impacts of material extraction.** For conventionally mined ore and
615 brine, energy consumption, CO₂-eq emission, and water consumption values are separated for the
616 material extraction processes found in the GREET model. For the circular extraction case, LCO-
617 based smartphones are assumed to be collected and transported to existing private and municipal
618 collection facilities (CFs) from each census block group in CA, assuming every person owned a
619 cell phone and purchased a new phone every three years. A shortest-route algorithm was used for

620 collection at the closest municipal collection facility determined by *k*-means clustering (**Note 4** in
621 **Supplementary Information**).

622 **Estimating environmental impacts of material transport.** In the conventional supply chain, a
623 network model of primary transport routes is established that connects mines to refinery locations
624 for Li, Co, Ni, and Al on a country-level basis (**Tables S8–S15**) because the amount of mined
625 material transported from each mine to each refinery was not known. The distances of the shortest-
626 path routes are calculated between mines and refineries by country, predicated on the closest
627 available modes of transport (including road, rail, and maritime). A major mine cluster or refinery
628 location was selected to represent country-level transport values (**Tables S14–S15**) based on
629 production volumes, and distances are quantified between international destinations. These
630 distances are used to calculate the energy consumption, CO₂-eq emission, and water consumption
631 associated with transportation of critical materials as mined concentrate. Mined concentrate is ore
632 or brine that is concentrated locally beyond natural concentration values to reduce weight for
633 transport to a refinery. By considering the total elemental mass and elemental weight percentage
634 of the mined concentrate transported along a route (**Tables S14–15**), the environmental impacts
635 on a per-element basis are calculated as a global weighted average (**Table S11**) with additional
636 process details in **Supplementary Information**.

637 For the circular case applied to California, end-of-life EV NCA LIBs are aggregated at one
638 CF per county closest to its centroid, where county-level data was the most granular data available.
639 All smartphones are aggregated at their nearest CFs. Aggregated smartphone and EV batteries are
640 assumed transported via truck to a single recycling facility located at the gravity point of
641 California's population based on census block-level data (detailed in **Note 4** in **Supplementary**
642 **Information**). The mass-distances traveled are converted to energy consumption, CO₂-eq
643 emission, and water consumption (**Table S8–S9**).

644 **Summary of study limitations.** Limitations based on key assumptions of supply chain steps
645 (extraction, transport, refinement) in each supply chain (conventional and circular) are briefly
646 discussed in this section.

647 *Extraction.* Mining data in conventional supply chains in GREET often only refer to one
648 mining country per material, meaning the global supply chain is not well captured. Transport
649 required between mining unit processes (e.g., crushing, flotation, and concentration) prior to

650 refinement is excluded from the analysis due to the lack of information in GREET. In collection
651 of end-of-life batteries in smartphones, inefficient transport to a CF (e.g., driving each smartphone
652 individually or taking longer transport routes to a CF) is not considered. In addition, all end-of-life
653 EV battery packs are assumed to be driven to each CF in their original vehicles, which is attributed
654 to the “product use” stage instead of extraction in life cycle assessment; therefore, zero CO₂-eq
655 emissions are assumed for the extraction step of EV batteries.

656 *Transport.* An inter-country LIB material transportation assessment is performed as a
657 weighted distribution between all major mining and refining countries. Results are sensitive to the
658 weight percentage of critical material in transported concentrate found in **Tables S14-S15**.
659 Transport between a domestic mine and refinery is not considered, resulting in net zero use of
660 resources in such cases. The resources required to separate an embedded battery from its device
661 prior to a refinement facility is not considered in a circular supply chains. Similarly, the effect of
662 transporting only LIBs separated from the devices is not considered. Incorporating the domestic
663 transport and separation operations can increase environmental impacts.

664 *Refinement.* Refinement data in conventional supply chains are limited to the country
665 scenarios reported in GREET, and transport between refinement unit processes is not included.
666 Ancillary processes (e.g., transport between unit processes) beyond direct refinement unit
667 processes and embodied resources of the capital equipment used for material refinement are not
668 considered for the circular supply chain. The chemical formats of output products differ between
669 the conventional and circular supply chains, but converting them to the same products will not
670 substantially change the results due to the similarity between the cathode salts of the two supply
671 chains (**Note 3 in Supplementary Information**).

672 **References**

- 673
- 674 1 Gielen, D. *et al.* World energy transitions outlook: 1.5° c pathway. (2021).
 - 675 2 Office, V. T. National blueprint for lithium batteries 2021–2030. (Vehicle Technologies
676 Office, 2021).
 - 677 3 Agency, I. E. (International Energy Agency Paris, France, 2021).
 - 678 4 Winslow, K. M., Laux, S. J. & Townsend, T. G. A review on the growing concern and
679 potential management strategies of waste lithium-ion batteries. *Resources, Conservation*
680 *and Recycling* **129**, 263-277 (2018).
 - 681 5 Staub, C. *MRF operator: Lithium-ion batteries are ‘ticking time bombs’*, <[https://resource-
682 recycling.com/recycling/2021/04/13/mrf-operator-lithium-ion-batteries-are-ticking-time-
683 bomb](https://resource-recycling.com/recycling/2021/04/13/mrf-operator-lithium-ion-batteries-are-ticking-time-bomb)> (2022).

- 684 6 Mayyas, A., Moawad, K., Chadly, A. & Alhseinat, E. Can circular economy and cathode
685 chemistry evolution stabilize the supply chain of Li-ion batteries? *The Extractive Industries*
686 *and Society* **14**, 101253 (2023).
- 687 7 Jacoby, M. in *Chemical & Engineering News* (American Chemical Society, 2019).
- 688 8 Ciez, R. E. & Whitacre, J. F. Examining different recycling processes for lithium-ion
689 batteries. *Nature Sustainability* **2**, 148-156 (2019).
- 690 9 Gaines, L., Dai, Q., Vaughey, J. T. & Gillard, S. Direct recycling R&D at the ReCell center.
691 *Recycling* **6**, 31 (2021).
- 692 10 Baum, Z. J., Bird, R. E., Yu, X. & Ma, J. Lithium-Ion Battery Recycling— Overview of
693 Techniques and Trends. *ACS Energy Lett.* (2022).
- 694 11 Crenna, E., Gauch, M., Widmer, R., Wäger, P. & Hischer, R. Towards more flexibility
695 and transparency in life cycle inventories for Lithium-ion batteries. *Resources,*
696 *Conservation and Recycling* **170**, 105619 (2021).
- 697 12 Wang, M. The greenhouse gases, regulated emissions, and energy use in transportation
698 (GREET) 2021. *Center for Transportation Research, Argonne National Laboratory* (2021).
- 699 13 Steward, D., Mayyas, A. & Mann, M. Economics and challenges of Li-ion battery
700 recycling from end-of-life vehicles. *Procedia Manufacturing* **33**, 272-279 (2019).
- 701 14 Kartini, E., Fakhrudin, M., Astuti, W., Sumardi, S. & Mubarak, M. Z. 1 edn 070001 (AIP
702 Publishing LLC).
- 703 15 Yang, Y., Xu, S. & He, Y. Lithium recycling and cathode material regeneration from acid
704 leach liquor of spent lithium-ion battery via facile co-extraction and co-precipitation
705 processes. *Waste Management* **64**, 219-227 (2017).
- 706 16 Makuza, B., Tian, Q., Guo, X., Chattopadhyay, K. & Yu, D. Pyrometallurgical options for
707 recycling spent lithium-ion batteries: A comprehensive review. *Journal of Power Sources*
708 **491**, 229622 (2021).
- 709 17 Kim, S. *et al.* A comprehensive review on the pretreatment process in lithium-ion battery
710 recycling. *Journal of Cleaner Production* **294**, 126329 (2021).
- 711 18 Balachandran, S. *et al.* Comparative study for selective lithium recovery via chemical
712 transformations during incineration and dynamic pyrolysis of EV Li-ion batteries. *Metals*
713 **11**, 1240 (2021).
- 714 19 de Chalendar, J. A., Taggart, J. & Benson, S. M. Tracking emissions in the US electricity
715 system. *Proc. Natl. Acad. Sci. U.S.A.* **116**, 25497-25502 (2019).
- 716 20 de Chalendar, J. A. & Benson, S. M. A physics-informed data reconciliation framework
717 for real-time electricity and emissions tracking. *Appl. Energy* **304**, 117761 (2021).
- 718 21 Grubert, E. & Sanders, K. T. Water use in the United States energy system: a national
719 assessment and unit process inventory of water consumption and withdrawals. *Environ.*
720 *Sci. Technol.* **52**, 6695-6703 (2018).
- 721 22 Bureau, U. S. C. <<https://www.census.gov/data.html>> (2022).
- 722 23 Energy, U. S. D. o. *Electric Vehicle Registrations by State,*
723 <<https://afdc.energy.gov/data/10962>> (2022).
- 724 24 CalRecycle. *Where to recycle: Map of public recycling locations,*
725 <<https://www2.calrecycle.ca.gov/wheretorecycle/>> (2022).
- 726 25 Roithner, C., Cencic, O. & Rechberger, H. Product design and recyclability: How statistical
727 entropy can form a bridge between these concepts-A case study of a smartphone. *Journal*
728 *of Cleaner Production* **331**, 129971 (2022).

729 26 Harper, G. *et al.* Recycling lithium-ion batteries from electric vehicles. *nature* **575**, 75-86
730 (2019).

731 27 Transportation, D. o. Hazardous Materials: Transportation of Lithium Batteries. (2014).

732 28 Sun, M., Yang, X., Huisingh, D., Wang, R. & Wang, Y. Consumer behavior and
733 perspectives concerning spent household battery collection and recycling in China: a case
734 study. *Journal of Cleaner Production* **107**, 775-785 (2015).

735 29 Daily, G. C. & Ruckelshaus, M. (Nature Publishing Group, 2022).

736 30 Berger, K., Schögl, J.-P. & Baumgartner, R. J. Digital battery passports to enable circular
737 and sustainable value chains: Conceptualization and use cases. *Journal of Cleaner*
738 *Production* **353**, 131492 (2022).

739 31 International Organization for, S. *Environmental management: life cycle assessment;*
740 *Principles and Framework.* (ISO, 2006).

741 32 Wernet, G. *et al.* The ecoinvent database version 3 (part I): overview and methodology.
742 *The International Journal of Life Cycle Assessment* **21**, 1218-1230 (2016).

743 33 Korolev, I. *et al.*

744 34 Brückner, L., Frank, J. & Elwert, T. Industrial recycling of lithium-ion batteries—A critical
745 review of metallurgical process routes. *Metals* **10**, 1107 (2020).

746 35 Bae, H. & Kim, Y. Technologies of lithium recycling from waste lithium ion batteries: a
747 review. *Materials advances* **2**, 3234-3250 (2021).

748 36 Solvay. Battery Recycling
749 . (Solvay, 2023).

750 37 Li-Cycle.
751

1
2
3
4
5
6
7
8
9
10
11
12
13
14
15
16
17
18

Supplementary Information

Life cycle comparison of industrial-scale lithium-ion battery recycling and mining supply chains

Michael L. Machala^{a,c,#}, Xi Chen^{b,#}, Samantha P. Bunke^{b,#}, Gregory Forbes^a, Akarys Yegizbay^d,
Jacques de Chalendar^a, Inês L. Azevedo^{a,c}, Sally Benson^{a,c}, William A. Tarpeh^{b,c,*}

^a*Department of Energy Resources Engineering, Stanford University, Stanford, California, 94305, United States*

^b*Department of Chemical Engineering, Stanford University, Stanford, California 94305, United States*

^c*Precourt Institute for Energy, Stanford University, Stanford, California 94305, United States*

^d*Department of Physics, Department of Economics, Kenyon College, Gambier, Ohio 43022, United States*

denotes equal co-first author contribution

* Corresponding author: email: wtarpeh@stanford.edu

Number of Pages: 33
Number of Tables: 15
Number of Figures: 7

19 **Supplementary Note 1. Drivers for recycling lithium-ion batteries**

20 *Projected LIB growth and supply*

21 Historic and projected values for global lithium-ion battery production by year are shown
22 in **Fig. S1**. Average values are presented as stacked bars by category and uncertainties represent
23 minimum and maximum reported values that highlight the range in uncertainty of projections. In
24 all projections, electric vehicles comprise the majority of LIB growth in the 2020s. The variation
25 in reported values is due, in part, to data selection and availability, such as including plug-in hybrid
26 electric vehicles in some projections while only considering fully electric vehicles in others.

27 Projected major supply-demand deficits of critical materials are extracted from industry
28 reports and other sources¹⁻⁷. The years where the supply-demand gap falls below zero and does
29 not recover to a positive value is shown in **Fig. S1** for Li, Ni, Co, and Cu. The range of deficit
30 years shows the supply and demand uncertainty of these critical elements, while the nearness of
31 these years to the publication date of this manuscript highlights the immediacy of supply risk and
32 deficit concerns.

33 *Embodied value of recycled materials*

34 Economic value ranges for commonly recycled commodities (i.e., glass, paper, plastic, and
35 metal cans) in **Fig. 1a** are based on historic monthly values in the U.S. from January 2018 to
36 December 2021 considering inflation⁸. 90% confidence intervals, represented by uncertainty bars,
37 show variation in pricing not only based on time, but also based on commodity variety in each
38 category. Because their constituent elements can be reused indefinitely, metal cans experience
39 recycling rates between 55–70%, whereas single-use plastic products are much lower at 3–30%.
40 Fundamentally, carbon atoms have minimal intrinsic economic value due to abundance and the
41 degradation of carbon-carbon bonds over multiple recycles.

42 Historic monthly LIB-relevant elemental value data is extracted from online databases⁹,
43 and weighted by the composition of EV 27-kWh battery packs provided by GREET¹⁰. Values are
44 also adjusted for inflation based on Dec 2021 USD. The relative composition of cathode powder
45 in smartphone batteries is taken from literature¹¹, and used to estimate the composition of an LCO-
46 based smartphone battery. In both cases, the entire mass of the battery or battery pack is not
47 included in reported recoverable value, only those elements shown in the figure. The reported
48 values are weighted by their proportion per kg of battery or battery pack. As such, additional
49 recoverable material (i.e., graphite, battery management system components) may still add
50 additional economic value but are not considered here. Note that, by March 2022, prices for many
51 critical elements were near or exceeding their 90% confidence maximum, while lithium carbonate
52 prices had nearly doubled.

53

54 **Supplementary Note 2. Emissions and water embodied in electricity consumption**

55 The year 2019 was chosen as the reference year for electricity consumption to remove any
56 major anomalies caused by the SARS-CoV-2 pandemic. For each environmental impact category
57 (energy, criteria air pollutants, and water), environmental impact conversion factors were used to
58 calculate total impacts of electricity in each balancing area based on the composition of different
59 electricity sources (e.g., natural gas, solar, hydroelectric). Total electricity production and
60 consumption in each balancing area, as well as exchanges with other balancing areas, were then
61 used to compute the environmental intensities embodied in electricity consumption for each
62 balancing area. This calculation generalizes an approach that was previously developed for CO₂,
63 SO₂ and NO_x¹²⁻¹⁴, and now incorporates additional data sources for electricity-embodied water¹⁵
64 and criteria air pollutants (SO_x, PM_{2.5}, PM₁₀, CO, CH₄, N₂O)^{15,16} Results of environmental
65 intensities are summarized as an electricity life cycle inventory in **Table S4**, and the original data
66 sources are detailed in **Supplementary Data Files A and B**.

67 **Supplementary Note 3. Environmental Intensity Differences**

68 *Compounds: Lithium carbonate versus Lithium sulfate*

69 Because many studies use lithium carbonate (Li₂CO₃) as a reference compound as opposed
70 to lithium sulfate (Li₂SO₄, the primary reference compound in this manuscript), the environmental
71 intensities of both are compared for the reductive calcination pathway (RC+Me+Hy) and the
72 hydrometallurgy pathway (Me+Hy) for energized LIBs. The results of this sensitivity analysis can
73 be found in **Fig. S3a** and show that relative to Li₂SO₄, the production of Li₂CO₃ exhibits higher
74 energy consumption intensity 3.9–28.8%, CO₂-eq emissions intensity 6.4–29.3%, and water
75 consumption intensity 2.1–21.9%.

76 *Pathways: Explaining discrepancies in literature of similar pathways*

77 Few previous studies have quantified the environmental impacts of recycling NCA LIBs.
78 Results from a previous study assessing the CO₂-eq emissions of different prevailing circular
79 refinement pathways are compared to the results from the current study¹⁷ (visualized in **Fig. S3c**).
80 After normalizing the literature data by the same functional unit as in the current study, the
81 previous study reports 7.53 ± 0.30 kg CO₂-eq/ kg NCA-eq, which is 48% lower than our result
82 (14.5 kg/kg NCA-eq). This discrepancy is due to the inclusion of recycled elemental inputs for
83 refinement into their analysis rather than considering only mined material¹⁷.

84 CO₂-eq emissions of prevailing circular refinement pathways, including pyrometallurgy
85 (Py), hydrometallurgy (Hy), and direct recycling (direct), are summarized in **Fig. S3c**. A
86 mechanical and hydrometallurgy refinement pathway (Me+Hy) used to recycle energized batteries
87 (recycled battery) is analyzed to model the existing circular refinement pathway in industries. In
88 general, the Me+Hy pathway in Redwood exhibits 66.2% higher CO₂-eq emissions than literature
89 values¹⁷. Because the embodied CO₂-eq emissions are similar to the electricity used in the two
90 studies (483 kg CO₂-eq/MWh in this study, and 510 CO₂-eq/MWh in the previous study), we
91 postulate that the different environmental intensities can be attributed to the different chemical
92 formulations of products in the two studies. While the previous study considered aqueous-phase

93 metal salts as the final products, subsequent crystallization or precipitation of metal compounds
94 will substantially increase the environmental intensities. For example, alkali consumables used for
95 metal precipitation contribute 24.3% to the overall CO₂-eq emissions of the Me+Hy pathway. The
96 component contributions in **Fig. S3b** indicate that electricity is a principal contributor (59.8%) to
97 CO₂-eq emissions in the Me+Hy pathway, implying that using electricity with lower CO₂-eq
98 intensity can further decarbonize the prevailing circular refinement pathways.

99

100 **Supplementary Note 4. Environmental intensities of upstream material extraction**

101 Two different methods for extracting battery-grade cathode materials are compared:
102 mining natural ore and brine, and collecting end-of-life LIBs per the comparison of functionally
103 equivalent process steps depicted in **Fig. 1b** of the main manuscript. The environmental intensities
104 of mining are based on GREET 2021 and are summarized in **Table S1**. Note that transportation of
105 material between mining locations and subsequent refinement steps are often excluded in GREET,
106 and production pathways incorporating transportation in between refining stages were modified
107 by subtracting the associated environmental intensities of the transportation steps (**Table S9**).
108 Relevant values can also be found in **Supplementary File A**.

109 To estimate the emissions of collecting end-of-life energized LIBs from consumers for
110 transport to a recycling facility for refinement, a transportation logistics model is established for
111 the state of California, U.S. As a model system, California (CA) was chosen because it is the most
112 populated US state (39.6 million, 2022) and has the highest number of electric vehicles,
113 representing 42% of the entire country in 2020¹⁸. Existing Collection Facilities (CFs) are provided
114 by the California Department of Resources Recycling and Recovery (CalRecycle)¹⁸. Two different
115 LIB products are considered: end-of-life LCO-based smartphones and end-of-life NCA-based EV
116 batteries. The assumed mass of transported smartphones and EV battery packs along with the mass
117 of active cathode material is summarized in **Table S10**.

118 In the first scenario, transport of smartphones from the census-block level to the nearest
119 CF is used to estimate environmental intensities of extraction from consumers. Population in every
120 census block is obtained from the U.S. Census Bureau¹⁹. It is assumed that one smartphone is
121 owned by each person in CA and is recycled every three years. To determine the closest CF, *k*-
122 means clustering is used for the allocation of census blocks to CFs based on minimizing the
123 distance between a census block's centroid and a singular CF, for all census blocks. This process
124 produces clusters of block groups whose LIB-embedded smartphones are allocated to the closest
125 CF. The distance from the census blocks to the CFs is determined by the shortest route using
126 Dijkstra's algorithm. The number of clusters, "*k*," used in this algorithm is fixed and equals the
127 total number of CFs. The relative size of a CF in the inset of **Fig. 4** indicates the number of
128 collected smartphones as compared to nearby CF clusters, and the smartphone collection area is
129 color-coded for distinction for each CF. Multiplying the resulting distances with the average mass
130 of a smartphone yields a mass-distance product (i.e., kg × km), which are converted to

131 environmental intensities using values for trucking (**Table S12**). Note that the shortest-route value
132 represents a lower bound of emissions.

133 In the second scenario, the number of registered zero-emission EVs in each CA county in
134 2012 is obtained from the California Energy Commission²⁰. All EV batteries are assumed to be
135 NCA-based and to reach end-of-life in 2019 (the reference year of this study). Because there is
136 more than one CF per county in some situations, the CF that was closest to the centroid of that
137 county was selected to represent the entire county. Additionally, because the distribution of EVs
138 within each county was not known beyond the county-level, it is assumed that LIB collection
139 occurred when an EV was driven to the CF for LIB extraction. The driving of an EV is considered
140 a separate step in the use of an EV and is excluded from the recycling lifetime; therefore, the
141 environmental intensities associated with driving to a CF are assumed zero. However, the removal
142 of EV batteries from a vehicle requires additional resources, and additional investigation is
143 required for quantifying these environmental intensities.

144 **Supplementary Note 5. Environmental intensities of upstream material transport**

145 *Mined concentrate transport*

146 A network model is used to determine the routes employed for transporting concentrated
147 mined material from mining to refinement locations. The resulting mass-distance values are
148 converted to environmental intensities using cradle-to-wheel fuel consumption data (**Table S12**).
149 For the critical LIB materials Li, Co, Ni, and Al, the contributions of material transported from
150 mines to refineries are associated with and aggregated based on the countries in which they are
151 extracted or refined, respectively (**Tables S14–S15**). The allocation of mined concentrate from
152 mines to refineries is based on a weighted distribution because data detailing the transported
153 amount and destination of material from every mine to every refinery was not accessible. Mined
154 materials from each extraction country are often concentrated domestically and then transported
155 to countries where they are refined, with allocation weighted by the amount of refinement being
156 performed relative to other refinery countries. The locations used to represent where the mines and
157 refineries are situated are determined based on where most extractive and refinement activity takes
158 place (indicated by latitude and longitude coordinates). The locations are incorporated into the
159 network model as the basis of origins and destinations of the routes employed for transportation
160 logistics.

161 Specific transit routes are chosen for the network model, including road (i.e., by truck), rail
162 (i.e., by train), and maritime (i.e., by shipping vessel) transport, exhaustive of the major routes
163 available worldwide²¹⁻²⁴. A portion of the network model and routes considered are presented in
164 **Fig. S5**. The ports associated with maritime transport connect all major sea ports to the closest rail
165 junction. Extraction of Co in the Democratic Republic of the Congo (DRC) is a unique case, where
166 logistics are limited to the road network for the transport of ores or brines from mines to a port²⁵.
167 The port in Beira, Mozambique is a major port for which mined Co from the DRC is transported
168 for refining. The maritime network connects the port in Beira, Mozambique to the closest road

169 junction to bridge the activity in the network model²⁶. For a particular element, the shortest route
 170 utilizing all combinations between mines and refineries is calculated with Dijkstra's algorithm²⁷.

171 The normalized mass-based environmental intensities of LIB material concentrate
 172 transported, $\bar{e}_{\text{Mat},i}^m$, are calculated by Eq. S1, where $e_{\text{Mat},i}^m$ is mass-based environmental intensities
 173 of the material i with a certain transport model (**Table S9**), d_i is the segmental transport distance
 174 in the shortest-route model, n_d is the total segments along that route, and w_i is the element weight
 175 percent from the country of origin.

$$176 \quad \bar{e}_{\text{Mat},i}^m = \frac{\sum_{i=1}^{n_d} (e_{\text{Mat},i}^m d_i)}{w_i} \quad (\text{S1})$$

177 Environmental intensities with weighted distributions, $E_{\text{Mat},i}$, for each element i are calculated to
 178 consider all routes for the three environmental intensities:

$$180 \quad E_{\text{Mat},i} = \sum_{i=1}^{n_d} (\bar{e}_{\text{Mat},i}^m m_i) \quad (\text{S2})$$

181 where m_i denotes the global percentage of an element considered for mined production or
 182 refinement production in 2019 (values summarized in **Tables S9–S10**). Environmental intensities
 183 per kg of embodied element are in **Table S12**. Lastly, these values of $E_{\text{Mat},i}$ are converted to LCO-
 184 eq and NCA-eq bases for comparison in **Fig. 5** in the main manuscript.

185 *Formulations for life cycle impacts of fuel use by different transport mode*

186 Life cycle inventories are developed for road, rail, and maritime modes of transport based
 187 on their use of fuel. The fuel used for each mode of transport is a composition of gasoline, diesel,
 188 and residual fuel oil, where the exact proportions (ϕ_j) are shown in **Table S13**. Volumetric
 189 environmental intensities (e_i) for fuel j were acquired for “cradle-to-tank” and “tank-to-wheel”
 190 portions of the life cycle regarding energy consumption, CO₂-eq emissions, and water
 191 consumption, as shown in **Table S12**. Efficiency factors (ξ_j) are employed to convert these
 192 volumetric properties to a mass-length basis (**Table S13**). All aforementioned values are used to
 193 develop life cycle inventories for the environmental intensities of fuel for rail, road, and maritime
 194 modes of transport on a per-unit-mass-distance basis:

$$196 \quad E_{\text{Fuel}} = \frac{\sum_{j=1}^n (e_{\text{Fuel},j}^v \phi_j)}{\xi_j} \quad (\text{S3})$$

197 These results are summed for each fuel type proportionally for each mode of transport, producing
 198 the life cycle inventories for the entire life cycle (**Table S12**).

199 *Collected smartphones and EV battery packs*

200 Environmental intensities of transportation of extracted LCO-based smartphones and
 201 NCA-based EV battery packs from CFs to the central recycling facility are calculated as a weighted

202 distribution based on mass-distance. The mass and distance traveled were converted to energy
203 consumption, CO₂-eq emissions, and water consumption using conversion factors from **Table S12**
204 and later normalized per kg of NCA-eq and LCO-eq precursor by the fractional percentage of
205 active material contained in each transported product. Again, note that disassembly and extraction
206 of battery cells from smartphones or EV battery packs prior to transport to a LIB recycling facility
207 will alter calculated values.

208 **Supplementary Data**

209 **Table S1.** The gate-to-gate environmental intensities of conventional and circular LIB supply chains including energy consumption, criteria air
 210 pollutant emissions, and water consumption, for producing one kg of NCA-eq battery-grade materials ($\text{LiNi}_{0.80}\text{Co}_{0.15}\text{Al}_{0.05}\text{O}_2$). The conventional
 211 supply chain is based on the GREET 2021 model¹⁰. Circular refinement includes reductive calcination (RC), mechanical (Me), and
 212 hydrometallurgical (Hy) steps, dealing with the recycled scrap and energized batteries. Note that the RC step is only required in recycled battery
 213 feedstocks. All circular data are based on power sources from Nevada Power Company (NEVP). The output products considered for conventional
 214 refinement are Li_2CO_3 , NiSO_4 , CoSO_4 , and Al_2O_3 ; the outputs produced by Redwood Materials are Li_2SO_4 , $(\text{Ni, Co})\text{SO}_4$ or as Al_2O_3 and $\text{Al}(\text{OH})_3$.
 215 Li_2CO_3 is also analyzed as a product for Redwood Materials. Data presented here are visualized in **Fig. 2** in the main manuscript, and **Fig. S3** below
 216 (note the comparison of Li_2SO_4 and Li_2CO_3 in Fig. S3a).

Supply chain	Element/Step	Energy (MJ/kg)	Criteria Air Pollutant Emission									Water (L/kg)	
			CO ₂	CH ₄	N ₂ O	CO	NO _x	SO _x	PM ₁₀	PM _{2.5}	CO ₂ -eq		
			(kg/kg)	(g/kg)	(mg/kg)	(g/kg)	(g/kg)	(g/kg)	(g/kg)	(g/kg)	(kg/kg)		
Conventional	Li	41.61	3.85	5.61	23.23	2.84	3.63	4.52	1.03	0.68	4.00	13.61	
	Ni	127.53	8.43	16.75	16.92	11.39	16.92	692.41	6.23	3.48	8.90	43.94	
	Co	24.56	1.50	3.45	35.60	3.45	1.75	35.60	5.83	0.70	1.59	16.69	
	Al	0.21	0.014	0.034	0.35	0.0089	0.016	0.020	0.012	0.0063	0.015	0.080	
Circular	Recycled scrap	Me	1.67	0.22	0.02	2.33	0.04	0.09	0.08	0.01	0.01	0.23	0.53
		Hy	20.31	2.62	1.04	96.48	0.63	0.87	4.06	0.17	0.14	2.68	8.46
		Total	21.98	2.85	1.06	98.81	0.67	0.96	4.14	0.18	0.15	2.91	8.99
	Recycled battery	RC	2.45	0.47	0.07	22.05	0.09	0.13	0.11	0.03	0.02	0.48	1.25
		Me	3.18	0.43	0.03	4.44	0.08	0.18	0.15	0.02	0.02	0.43	1.00
		Hy	38.7	5.52	0.83	50.58	1.23	2.13	8.47	0.35	0.30	5.56	17.79
		Total	40.35	6.42	0.93	77.07	1.40	2.44	8.73	0.40	0.34	6.46	20.04

217

218

219 **Table S2.** Life cycle inventory for consumables used in circular refinement steps. Data for all consumables are generated using the GREET 2021
 220 model and are normalized by 1 kg of each consumable²⁶. Data of natural gas are obtained by averaging U.S. natural gas production from shale and
 221 conventional methods²⁸. Total CO₂-eq are calculated by summing greenhouse gases multiplied by the corresponding global warming potential
 222 (GWP), with conversion factor global warming potentials (GWP) for 100 years: CO₂ (GWP = 1), CH₄ (GWP = 25), and N₂O (GWP = 298)²⁹.

Consumable	Energy (MJ/kg)	Water (L/kg)	CO₂ (kg/kg)	CH₄ (g/kg)	N₂O (g/kg)	CO (g/kg)	NO_x (g/kg)	SO_x (g/kg)	PM₁₀ (g/kg)	PM_{2.5} (g/kg)	CO₂-eq (kg/kg)
H ₂ SO ₄	0.19	0.29	0.011	0.026	0.00023	0.0053	0.0088	20.01	0.0011	0.00067	0.011
HCl	31.62	5.20	1.82	4.66	0.39	0.98	1.57	0.86	0.16	0.11	1.94
HNO ₃	12.05	5.06	0.67	2.10	4.77	1.51	1.45	0.21	0.027	0.025	2.15
H ₂ O ₂	17.49	2.10	0.99	2.46	0.016	0.35	0.53	0.30	0.063	0.048	1.06
Ca(OH) ₂	4.93	6.16	1.26	0.68	0.0012	0.46	0.26	0.14	0.14	0.10	1.28
NaOH	32.00	13.88	1.84	4.81	0.044	1.09	1.78	0.95	0.18	0.12	1.98
Natural gas	50.47	0.51	0.20	6.42	0.0014	0.51	0.57	0.48	0.017	0.015	0.36

223

224 **Table S3.** Relative contribution of different inputs and consumables in the circular refinement processes (for scrap and energized battery feedstocks)
 225 to the environmental intensities, including energy consumption, CO₂-eq emissions, and water consumption. The data are based on the GREET 2021
 226 model¹⁰ and are visualized in **Fig. 3a** in the main manuscript. “N/A” denotes “not applicable.”

Environmental impact	Recycling pathway	Reductive Calcination				Mechanical		Hydrometallurgy			
		Electricity input (%)	Water input (%)	Alkali (%)	CO ₂ emission (%)	Primary electricity (%)	Water input (%)	Primary electricity (%)	H ₂ SO ₄ (%)	H ₂ O ₂ (%)	Alkali (%)
Energy consumption	Recycled scrap	N/A	N/A	N/A	N/A	7.60	N/A	62.65	1.42	20.14	8.19
	Recycled battery	4.70	N/A	0.82	N/A	7.16	N/A	79.09	1.44	N/A	6.79
CO ₂ -eq emissions	Recycled scrap	N/A	N/A	N/A	N/A	1.83	N/A	15.05	2.00	31.13	49.99
	Recycled battery	4.36	N/A	1.56	1.47	6.64	N/A	73.25	0.63	N/A	12.10
Water consumption	Recycled scrap	N/A	N/A	N/A	N/A	9.87	0.53	81.38	1.27	2.18	4.77
	Recycled battery	3.29	0.67	2.26	N/A	5.01	8.27	55.33	6.13	N/A	19.03

227

228

229 **Table S4.** Environmental intensities of circular refinement steps using different electricity sources for producing one kg of NCA-eq battery-grade
 230 materials (LiNi_{0.80}Co_{0.15}Al_{0.05}O₂). Circular refinement includes reductive calcination (RC), mechanical (Me), and hydrometallurgical (Hy) steps,
 231 dealing with the production scrap and energized batteries. Note that the RC step is only required for energized batteries. Power sources are from
 232 Nevada renewable energy tariff (NV*), Bonneville Power Administration (BPAT), California Independent System Operator (CISO), and Western
 233 Area Power Administration–Colorado-Missouri (WACM)^{12,13}. Data presented here are visualized in **Fig. 3b** in the main manuscript.

Power sources	Recycling pathways	Step	Energy (MJ/kg)	Criteria Air Pollutant Emission									Water (L/kg)	
				CO ₂	CH ₄	N ₂ O	CO	NO _x	SO _x	PM ₁₀	PM _{2.5}	CO ₂ -eq		
				(kg/kg)	(g/kg)	(mg/kg)	(g/kg)	(g/kg)	(g/kg)	(g/kg)	(g/kg)	(g/kg)		(kg/kg)
NV*	Recycled scrap	Me	1.67	0.02	0	0	0	0	0	0	0	0.02	4.64	
		Hy	20.31	0.91	0.91	77.24	0.27	0.11	3.40	0.07	0.05	0.96	42.35	
		Total	21.98	0.93	0.91	77.24	0.27	0.11	0	0.07	0.05	0.98	46.99	
	Recycled Battery	RC	2.45	0.21	0.05	19.13	0.03	0.02	0.01	0.01	0.008	0.22	6.38	
		Me	3.18	0.03	0	0	0	0	0	0	0	0.03	8.83	
		Hy	38.73	1.17	0.50	1.55	0.30	0.19	6.80	0.09	0.07	1.18	104.14	
		Total	44.36	1.41	0.55	20.69	0.33	0.21	6.81	0.10	0.078	1.43	119.35	
		Recycled scrap	Me	4.30	0.06	0.005	0.70	0.01	0.03	0.03	0.004	0.003	0.06	3.22
			Hy	1.23	1.23	0.95	83.03	0.36	0.33	3.62	0.09	0.07	1.27	30.65
Total	1.28		1.29	0.95	83.73	0.37	0.36	3.65	0.09	0.08	1.33	33.87		
BPAT	Recycled scrap	RC	2.45	0.26	0.06	20.01	0.05	0.05	0.05	0.01	0.01	0.26	4.61	
		Me	3.18	0.10	0.009	1.34	0.02	0.05	0.05	0.006	0.005	0.10	6.12	
		Hy	38.73	1.97	0.60	16.32	0.54	0.75	7.37	0.15	0.12	1.99	74.32	
		Total	44.36	2.33	0.66	37.67	0.61	0.85	7.47	0.17	0.14	2.36	85.06	
CISO	Recycled scrap	Me	1.67	0.11	0.007	1.44	0.03	0.05	0.03	0.006	0.006	0.11	1.27	
		Hy	20.31	1.69	0.96	89.07	0.52	0.50	3.62	0.12	0.10	1.74	14.59	
		Total	21.98	1.80	0.97	90.51	0.55	0.55	3.65	0.13	0.11	1.85	15.86	

		RC	2.45	0.33	0.06	20.93	0.07	0.08	0.04	0.02	0.02	0.33	2.18
	Recycled	Me	3.18	0.21	0.01	2.73	0.06	0.09	0.05	0.01	0.01	0.21	2.42
	scrap	Hy	38.73	3.14	0.64	31.70	0.96	1.19	7.36	0.22	0.19	3.17	33.40
		Total	44.36	3.68	0.71	55.35	1.09	1.36	7.45	0.25	0.21	3.76	37.99
		Me	1.67	0.31	0.05	6.90	0.09	0.21	0.28	0.01	0.02	0.31	1.42
	Recycled	Hy	20.31	3.34	1.30	134.16	1.01	1.88	5.72	0.17	0.20	3.41	15.81
	scrap	Total	21.98	3.65	1.35	141.06	1.10	2.09	6.00	0.18	0.22	3.72	17.23
		RC	2.45	0.58	0.11	27.76	0.15	0.29	0.36	0.03	0.03	0.59	2.36
	Recycled	Me	3.18	0.59	0.09	13.14	0.17	0.41	0.54	0.02	0.04	0.60	2.70
	scrap	Hy	38.73	7.34	1.49	146.60	2.20	4.70	12.71	0.35	0.45	7.42	36.51
		Total	44.36	8.51	1.69	187.50	2.52	5.39	13.60	0.40	0.52	8.61	41.57

WACM

235 **Table S5.** Life cycle inventory of embodied emission of air pollutants and water consumption of different electricity sources. Total CO₂-eq values
 236 are calculated by summing greenhouse gases multiplied by the corresponding 100-year global warming potential (GWP), including CO₂ (GWP =
 237 1), CH₄ (GWP = 25), and N₂O (GWP = 298)²⁹. Electricity sources are balancing grids from Bonneville Power Administration (BPAT), California
 238 Independent System Operator (CISO), Nevada Power Company (NEVP), Western Area Power Administration–Colorado–Missouri (WACM), and
 239 a Nevada renewable energy tariff (NV*) comprised of 85% geothermal, 10% solar, and 5% hydropower. Alternative power generated by hydraulic,
 240 nuclear, solar, natural gas (Ng), wind, coal, oil, biomass, geothermal, and others are summarized in the lower sections. Data listed are visualized in
 241 Fig. S5. “N/A” denotes “not applicable”^{12,13}.

	Electricity source	Criteria Air Pollutant Emissions								CO ₂ -eq (g/MWh)	Water (L/kWh)
		CO ₂ (kg/MWh)	CH ₄ (kg/MWh)	N ₂ O (kg/MWh)	CO (kg/MWh)	NO _x (kg/MWh)	SO _x (kg/MWh)	PM ₁₀ (kg/MWh)	PM _{2.5} (kg/MWh)		
Balancing Areas	BPAT	118.57	0.010	0.0015	0.024	0.057	0.059	0.0066	0.0057	119.28	6.94
	CISO	239.30	0.014	0.0031	0.067	0.10	0.058	0.014	0.013	240.58	2.74
	NEVP	483.48	0.034	0.0050	0.095	0.20	0.17	0.027	0.024	485.83	1.14
	WACM	670.34	0.10	0.015	0.20	0.46	0.61	0.050	0.040	677.33	3.06
	NV*	36.56	N/A	N/A	N/A	N/A	N/A	N/A	N/A	36.56	10.00
Electricity generation sources	Hydro	20.50	N/A	N/A	N/A	N/A	N/A	N/A	N/A	20.50	9.53
	Nuclear	13.00	N/A	N/A	N/A	N/A	N/A	N/A	N/A	13.00	2.18
	Solar	43.40	N/A	N/A	N/A	N/A	N/A	N/A	N/A	43.40	0.31
	Nat. gas	489.28	0.010	0.0016	0.067	0.11	0.0071	0.021	0.021	490	0.26
	Wind	13.00	N/A	N/A	N/A	N/A	N/A	N/A	N/A	13.00	0.01
	Coal	990.20	0.16	0.023	0.30	0.71	0.94	0.076	0.060	1001	1.55
	Oil	837.23	0.013	0.0082	0.51	3.70	2.29	0.24	0.217	840	0.33
	Biomass	31.30	0.11	0.060	1.18	0.68	0.049	0.073	0.069	52	5.50
	Geotherm	36.70	N/A	N/A	N/A	N/A	N/A	N/A	N/A	36.70	11.17
	Others	58.96	0.00087	0.00013	0.0057	0.010	0.00060	0.002	0.0018	59	7.34

243 **Table S6.** The environmental intensities of the material extraction step for producing one kg of NCA-eq ($\text{LiNi}_{0.80}\text{Co}_{0.15}\text{Al}_{0.05}\text{O}_2$) mined natural
 244 material in the conventional supply chain. Impacts include energy consumption, criteria air pollutant emissions, and water consumption. The
 245 conventional extraction step is based on the GREET 2021 model¹⁰. Data presented are visualized in **Fig. 5** in the main manuscript.

Element	Energy (MJ/kg)	Criteria Air Pollutant Emissions									Water (L/kg)
		CO ₂ (kg/kg)	CH ₄ (g/kg)	N ₂ O (mg/kg)	CO (g/kg)	NO _x (g/kg)	SO _x (g/kg)	PM ₁₀ (g/kg)	PM _{2.5} (g/kg)	CO ₂ -eq (kg/kg)	
Li	8.25	0.58	0.74	7.56	0.33	1.22	0.047	0.057	0.048	0.60	5.35
Ni	26.06	1.95	2.59	97.78	1.31	6.53	3.93	0.52	0.40	2.00	7.77
Co	2.76	0.20	0.25	4.91	0.21	4.86	0.011	5.70	0.61	0.21	0.87
Al	2.0 × 10 ⁻³	1.5 × 10 ⁻⁴	1.8 × 10 ⁻⁴	3.4 × 10 ⁻³	1.1 × 10 ⁻⁴	4.3 × 10 ⁻⁴	8.1 × 10 ⁻⁵	2.4 × 10 ⁻³	1.2 × 10 ⁻³	1.6 × 10 ⁻⁴	0.016

246

247 **Table S7.** The environmental intensities of material extraction and refinement steps in conventional supply chains, including energy consumption,
 248 criteria air pollutant emissions, and water consumption. The values are normalized by one kg of each element regardless of material type (e.g., ore
 249 type or elemental concentration). The conventional material extraction and refinement steps are based on the GREET 2021 model¹⁰. Note that values
 250 of lithium are weight averages of 45% brine- and 55% ore-based lithium production³⁰. Refinement materials reference Li₂CO₃, NiSO₄, CoSO₄, Al₂O₃,
 251 and MnSO₄.

252

Step	Element	Energy (MJ/kg)	Criteria Air Pollutant Emissions									Water (L/kg)
			CO ₂ (kg/kg)	CH ₄ (g/kg)	N ₂ O (mg/kg)	CO (g/kg)	NO _x (g/kg)	SO _x (g/kg)	PM ₁₀ (g/kg)	PM _{2.5} (g/kg)	CO ₂ -eq (kg/kg)	
Extraction	Li	114.78	8.07	10.24	105.16	4.53	17.02	0.66	0.79	0.66	8.40	9.41
	Ni	53.30	3.98	5.31	200.00	2.68	13.36	8.05	1.06	0.81	4.20	15.89
	Co	29.97	2.18	2.68	53.39	2.31	5.28	0.12	61.89	6.66	2.30	9.41
	Al	0.14	0.01	0.01	0.24	0.01	0.03	0.01	0.17	0.09	0.01	1.12
	Mn	23.11	1.34	2.76	23.45	0.86	1.11	0.73	5.29	2.65	1.40	6.73
	Cu	4.06	0.25	0.45	3.32	0.26	0.45	0.10	0.08	0.04	0.26	0.95
Refinement	Li	579.22	53.60	78.09	323.40	39.56	50.48	62.97	14.27	9.48	55.60	189.37
	Ni	260.87	17.24	34.26	350.60	23.30	34.62	1416.30	12.75	7.12	18.20	89.88
	Co	266.79	16.26	37.44	386.77	11.22	19.04	64.16	63.33	7.60	17.30	213.94
	Al	15.18	0.98	2.42	24.63	0.63	1.15	1.41	0.89	0.45	1.00	5.66
	Mn	1.08	0.86	0.11	1.78	7.3E-02	0.57	3.84	4.1 × 10 ⁻²	3.6 × 10 ⁻²	0.86	0.57
	Cu	32.25	1.99	4.68	42.26	1.78	2.23	140.28	0.21	0.14	2.10	5.26

253

254

255 **Table S8.** Separated cradle-to-gate conventional and circular LIB supply steps showing energy consumption, greenhouse gas emissions, and water
 256 consumption for two different functional units: NCA-eq and LCO-eq cathode material salts. Conventional supply chain values reflect dominant
 257 global supply chains (excluding recycled feedstocks) extracted from GREET, with transport values modeled in this work. The circular supply chain
 258 represents recycling of NCA-based battery packs and LCO-based smartphones in California as described elsewhere in the study.

Supply chain	Step	Energy Consumption				CO ₂ -eq Emission				Water Consumption			
		NCA		LCO		NCA		LCO		NCA		LCO	
		Value (MJ/kg NCA-eq)	Percent age (%)	Value (kg/kg LCO-eq)	Percent age (%)	Value (kg/kg NCA-eq)	Percent age (%)	Value (kg/kg LCO-eq)	Percent age (%)	Value (L/kg NCA-eq)	Percent age (%)	Value (kg/kg LCO-eq)	Percent age (%)
Conventional	Extraction	37.1	14	26.2	10	2.85	14	1.96	9	14.0	15	10.9	7
	Transport	31.2	12	44.9	16	3.68	17	4.32	21	0.757	1	1.11	1
	Refinement	194	74	202	74	14.5	69	14.4	70	77.3	84	142	92
	Total	262	100	273	100	21.0	100	20.6	100	92.1	100	154	100
Circular	Extraction	0	0	0.385	0	0	0	0.0189	0.2	0	0	0.00920	0
	Transport	1.49	3.5	9.58	8	0.0729	2.2	0.470	5	0.036	0	0.229	0
	Refinement	44.4	97	112	92	3.72	98	9.40	95	38.0	99.9	96.1	99.8
	Total	45.8	100	122	100	3.79	100	9.89	100	38.0	100	96.3	100

259

260 **Table S9.** The estimated environmental intensities of transporting Li, Co, Ni, and Al concentrates of mined
 261 material in conventional supply chains normalized by the content of metal in transit (top table). The
 262 transportation impacts of aggregated LCO-based smartphones and NCA-based EV batteries are found in
 263 the bottom table from collection facilities to a recycling center positioned at the gravity point (i.e., center)
 264 of the California population. Data presented are visualized in **Fig. 5** in the main manuscript.
 265

Conventional Material Transport

Material Transported	Energy Consumption (MJ/t metal)	CO₂-eq Emissions (kg/t metal)	Water Consumption (L H₂O/t metal)
Li concentrate	37,808	6,152	964
Co concentrate	70,149	6,445	1,727
Ni concentrate	44,755	5,355	1,073
Al concentrate	10,770	1,809	278

Circular Material Transport

Product Transported	Energy Consumption (MJ/t product)	CO₂-eq Emissions (kg/t product)	Water Consumption (L/t product)
Smartphone Collection*	20.5	1.00	0.490
Smartphone Transport	510	25.0	12.2
EV Battery Transport	515	25.3	12.3

266 *Smartphone collection is a material extraction step but included here for reference. Collection is modeled by the transportation
 267 resources required for battery collection from consumer census block and transport to a collection facility; it does not include other
 268 potential steps such as device disassembly for battery extraction from products.
 269

270 **Table S10.** Mass of lithium-ion battery embedded products considered in this analysis^{10,11,31}.

Battery Type	Element	Assumed Mass (kg)
	LCO-battery embedded smartphone	0.118
LCO	Mass of battery per smartphone	0.026
	LCO active material per kg of battery	0.162
	End-of-life 27-kWh EV NCA battery pack	108
NCA	NCA active material per NCA battery pack	37.4

271
272

273 **Table S11.** Total metal extraction mass of ores or brines from global mining activity for Li, Co, Ni, and
274 Al in 2019³².
275

Element	Total Mined & Refined (t)
Li	86,000
Co	144,000
Ni	2,400,000
Al	189,000,000

276
277

278 **Table S12.** Environmental intensities of fuels use by different modes of transport in the stages of “cradle-
 279 to-wheel”, “cradle-to-tank”, and “tank-to-wheel”. Data are from references^{10,33,34}.

Transport Stage	Mode of Transport	Maritime	Rail	Road	Gasoline	Diesel	Residual Fuel Oil
Cradle-to-wheel	Energy Consumption (MJ/t km)	0.15	0.213	2.3	N/A	N/A	N/A
	CO ₂ -eq emissions (g/t km)	27.28	33.69	112.8	N/A	N/A	N/A
	Water Consumption (L/t km)	0.00396	0.00319	0.055	N/A	N/A	N/A
Cradle-to-tank	Energy Consumption (MJ/t km)	0.01	0.024	0.3	7.11	4.54	2.80
	CO ₂ -eq emissions (g/t km)	1.00	1.57	17.9	503	299	193
	Water Consumption (L/t km)	0.00396	0.00319	0.055	4.36	0.608	0.396
Tank-to-wheel	Energy Consumption (MJ/t km)	0.14	0.189	2.0	33.8	36.0	39.7
	CO ₂ -eq emissions (g/t km)	26.3	32.1	94.9	N/A	N/A	N/A
	Water Consumption (L/t km)	N/A	N/A	N/A	N/A	N/A	N/A

280
 281
 282
 283
 284
 285

286 **Table S13.** Proportions of different fuel use, ϕ , and fuel efficiency ζ , by different transport modes. ζ are
 287 obtained from references^{28,35-37}. Data presented are employed in eq. S3 for the visualization in **Fig. 5** in the
 288 main manuscript, and are quantified in **Table S8**.

Transport Mode	Fuel	Proportion of Fuel Use, ϕ (%)	Fuel Efficiency, ζ (t km/L)
Maritime	Gasoline	15.3	270.8
	Diesel	29.7	
	Residual Fuel Oil	55.1	
Rail	Gasoline	0	181.6
	Diesel	0	
	Residual Fuel Oil	100	
Road	Gasoline	9.9	18.7
	Diesel	89.4	
	Residual Fuel Oil	0	

289
 290
 291
 292
 293
 294

295 **Table S14.** Mine/mine cluster country with latitude and longitude used in analysis, mine capacity, and
 296 element weight percentage, for Li³⁸, Co³⁹, Ni⁴⁰, and Al⁴¹. Standard quantity is as reported and scaled
 297 quantity includes locations considered in the study scaled to 100%. References for all mine locations and
 298 assumed weight percentages of mined concentrates are obtained from the public repository⁴².

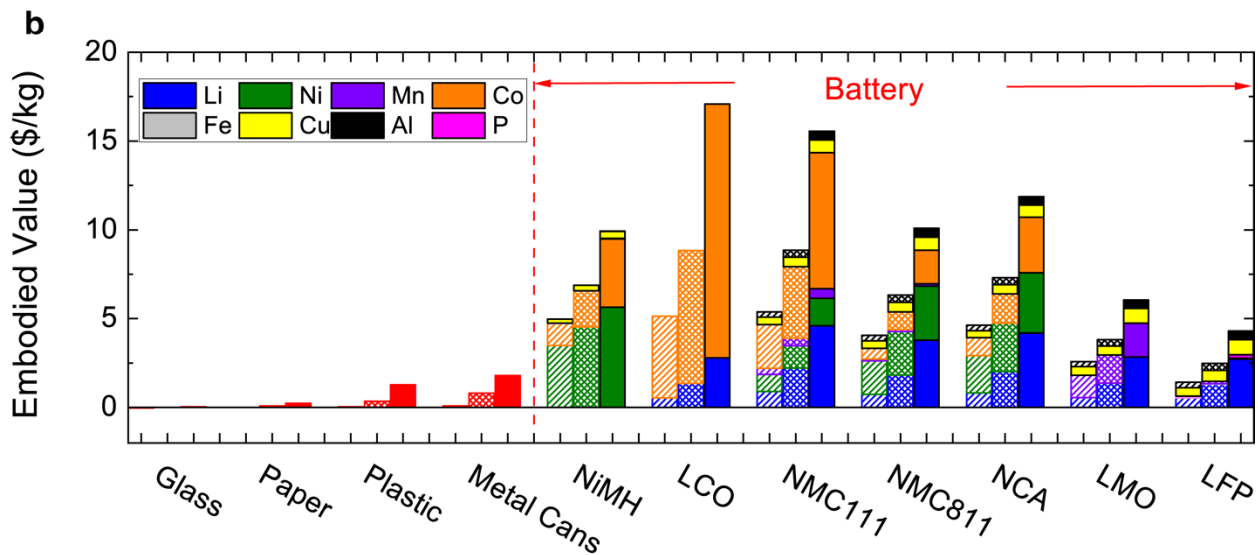
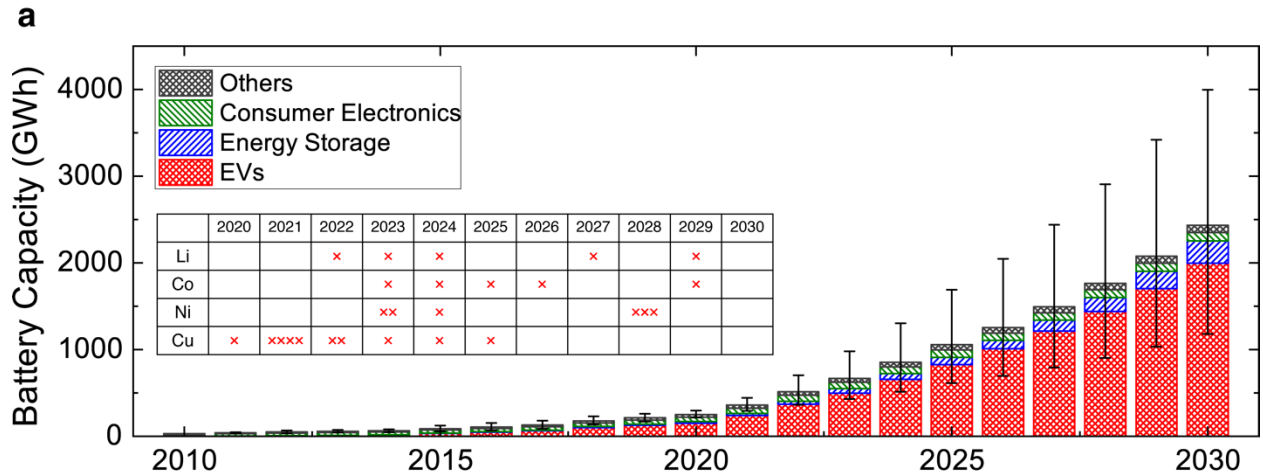
Element Type	Mine Location	Latitude-Longitude Coordinates for Analysis	Mine Capacity (% of total / scaled to 100%)	Mine Capacity (standard quantity / scaled by total)	Element Content (wt. % of element in transported concentrate)
Li	Australia	(-33.85, 116.06)	52.3% / 52.9%	45,000 / 45,529	3.7
	Chile	(-26.23, -69.12)	22.4% / 22.7%	19,300 / 19,527	18.8
	China	(36.62, 101.78)	12.6% / 12.7%	10,800 / 10,927	18.8
	Argentina	(-23.79, -66.76)	7.3% / 7.4%	6,300 / 6,374	18.5
	Brazil	(-20.06, -44.57)	2.8% / 2.8%	2,400 / 2,428	3.7
	Zimbabwe	(-17.37, 31.43)	1.4% / 1.4%	1,200 / 1,214	2.2
Co	Democratic Republic of Congo	(-8.75, 26.41)	69.4% / 80.4%	100,000 / 115,811	9.5 (5.0–14.0)
	Russia	(69.35, 88.21)	4.4% / 5.1%	6,300 / 7,296	12.5
	Australia	(-28.77, 121.88)	4.0% / 4.6%	5,740 / 6,648	3.0
	Philippines	(9.76, 125.51)	3.5% / 4.1%	5,100 / 5,906	4.9
	Cuba	(20.66, -74.95)	2.6% / 3.1%	3,800 / 4,401	5.0
	Madagascar	(-18.95, 48.30)	2.4% / 2.7%	3,400 / 3,938	4.2
Ni	Indonesia	(-1.43, 121.45)	25.3% / 35.1%	606,000 / 843,179	8.45
	Philippines	(9.48, 125.80)	14.4% / 20.0%	344,915 / 479,909	5.11
	Russia	(58.45, 92.19)	11.3% / 15.8%	272,000 / 378,457	9.45
	New Caledonia	(-22.37, 166.87)	9.0% / 12.5%	216,225 / 378,457	7.89
	Canada	(46.83, -71.25)	7.3% / 10.2%	175,761 / 244,551	15.7
	China	(30.66, 104.07)	4.6% / 6.4%	110,000 / 153,052	9.48
Al	Australia	(-31.95, 115.86)	29.3% / 34.1%	105,000 / 122,117	15.0
	China	(23.64, 108.27)	19.6% / 22.7%	70,000 / 81,411	24.3
	Guinea	(10.37, -13.58)	18.7% / 21.8%	67,000 / 77,922	23.8
	Brazil	(-1.46, -48.50)	9.5% / 11.0%	34,000 / 39,543	21.2
	Indonesia	(3.95, 108.14)	4.7% / 5.5%	17,000 / 19,771	21.2

Jamaica	(18.04, -77.51)	2.5% / 2.9%	9,020 / 10,490	23.8
Kazakhstan	(52.27, 77.00)	1.6% / 1.9%	5,800 / 6,746	23.0

300 **Table S15.** Refinery location (latitude and longitude) and refining capacity for Li, Co, Ni, and Al. Standard
 301 quantity is as reported by USGS and others; scaled quantity includes locations considered in the study
 302 scaled to 100%. References for all refinery locations are itemized and obtained from a public repository⁴².

Element	Refining Location	Latitude-Longitude Coordinates for Analysis	Refining Capacity (% of total / scaled to 100%)	Refining Capacity (standard quantity / scaled by total)
Li	China	(28.68, 115.88)	61.0% / 61.0%	52,306 / 52,306
	Australia	(-31.95, -115.86)	18.0% / 18.0%	15,403 / 15,403
	United States	(35.18, -81.34)	11.0% / 11.0%	9,627 / 9,627
	Chile	(-23.65, -70.40)	10.0% / 10.0%	8,664 / 8,664
Co	China	(24.72, 114.95)	67.0% / 75.3%	96,480 / 108,404
	Finland	(63.84, 23.13)	10.0% / 11.2%	14,400 / 16,180
	Canada	(50.00, -85.00)	5.0% / 5.6%	7,200 / 8,090
	Norway	(58.15, 8.00)	4.0% / 4.5%	5,760 / 6,472
	Japan	(33.96, 133.31)	3.0% / 3.4%	4,320 / 4,854
Ni	China	(27.99, 120.70)	23.3% / 23.3%	244,900 / 244,900
	Canada	(50.00, -85.00)	15.5% / 15.5%	163,200 / 163,200
	Russia	(69.35, 88.20)	15.0% / 15.0%	157,396 / 157,396
	Japan	(33.96, 133.31)	11.6% / 11.6%	121,750 / 121,750
	Australia	(-27.28, 120.55)	9.9% / 9.9%	103,900 / 103,900
	Norway	(58.15, 8.00)	8.2% / 8.2%	86,500 / 86,500
	Finland	(61.31, 22.14)	5.7% / 5.7%	59,700 / 59,700
	South Africa	(-25.65, 27.26)	4.6% / 4.6%	48,100 / 48,100
	Madagascar	(-18.86, 48.30)	3.4% / 3.4%	35,474 / 35,474
New Caledonia	(-22.28, 167.02)	2.9% / 2.9%	30,875 / 30,875	
Al	China	(36.07, 119.16)	54.5% / 63.1%	195,150 / 225,971
	Australia	(-32.82, 151.71)	15.2% / 17.6%	54,373 / 62,960
	Brazil	(-2.53, -4.30)	6.5% / 7.6%	23,418 / 27,116
	India	(21.85, 84.03)	6.5% / 7.6%	18,008 / 20,852
	Russia	(61.67, 50.82)	5.0% / 5.8%	7,429 / 8,602
	Jamaica	(17.96, -77.60)	2.1% / 1.9%	5,841 / 6,764

Saudi Arabia	(27.49, 49.14)	1.4% / 1.6%	4,953 / 5,735
--------------	----------------	-------------	---------------

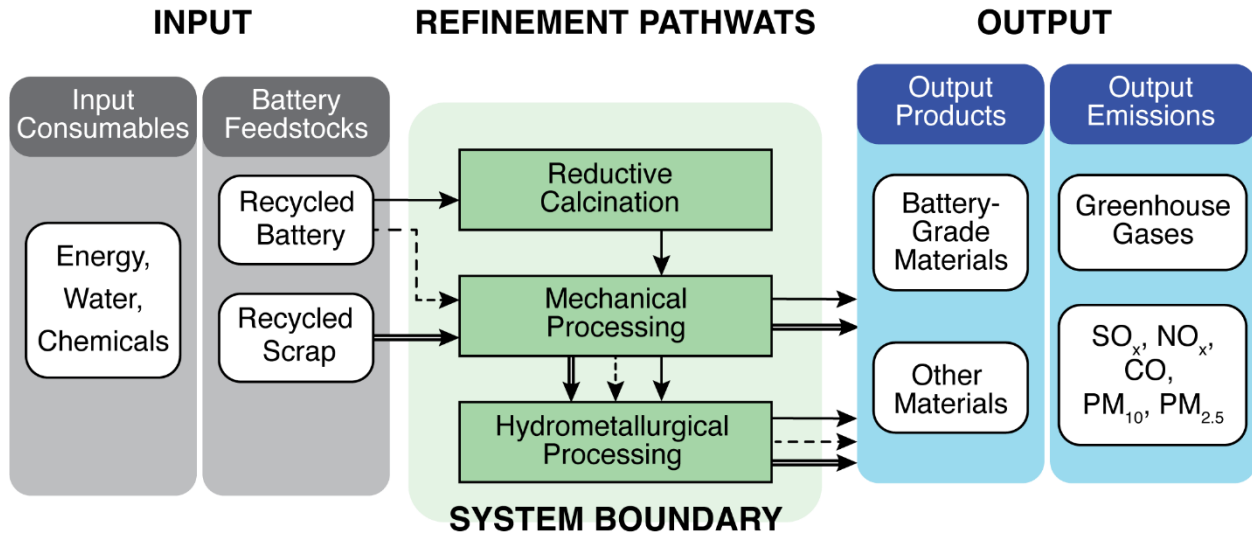


Commodity Recycled

304 **Fig. S1 | a**, Projected global demand of lithium-ion batteries in representative industries including
 305 electric vehicles (EVs), energy storage, consumers electronics, and others. The uncertainty bars
 306 indicate the range of projections by different reports, highlighting varying optimism in supply and
 307 production capacity, along with methods of quantification, where hybrid or plug-in EVs may not
 308 be included in some analyses. Inset presents a compilation of industry report projections of when
 309 global supply-demand gaps will become negative and will not recover to positive values, running
 310 a supply deficit. Each “x” denotes a literature estimate⁴³⁻⁴⁶. **b**, composition breakdown of the
 311 embodied value of each commodity. Glass, paper, plastic, and metal cans are an average of three
 312 to five major sub-categories. The center bar for each commodity is the average value adjusted for
 313 inflation between January 2018 and December 2021 and in December 2021 USD^{1-7,47}. The side
 314 bars represent the 90% confidence interval of those commodity values. Notably, all batteries
 315 chemistries represent 27-kWh battery packs with breakdowns provided by GREET 2021. LCO is

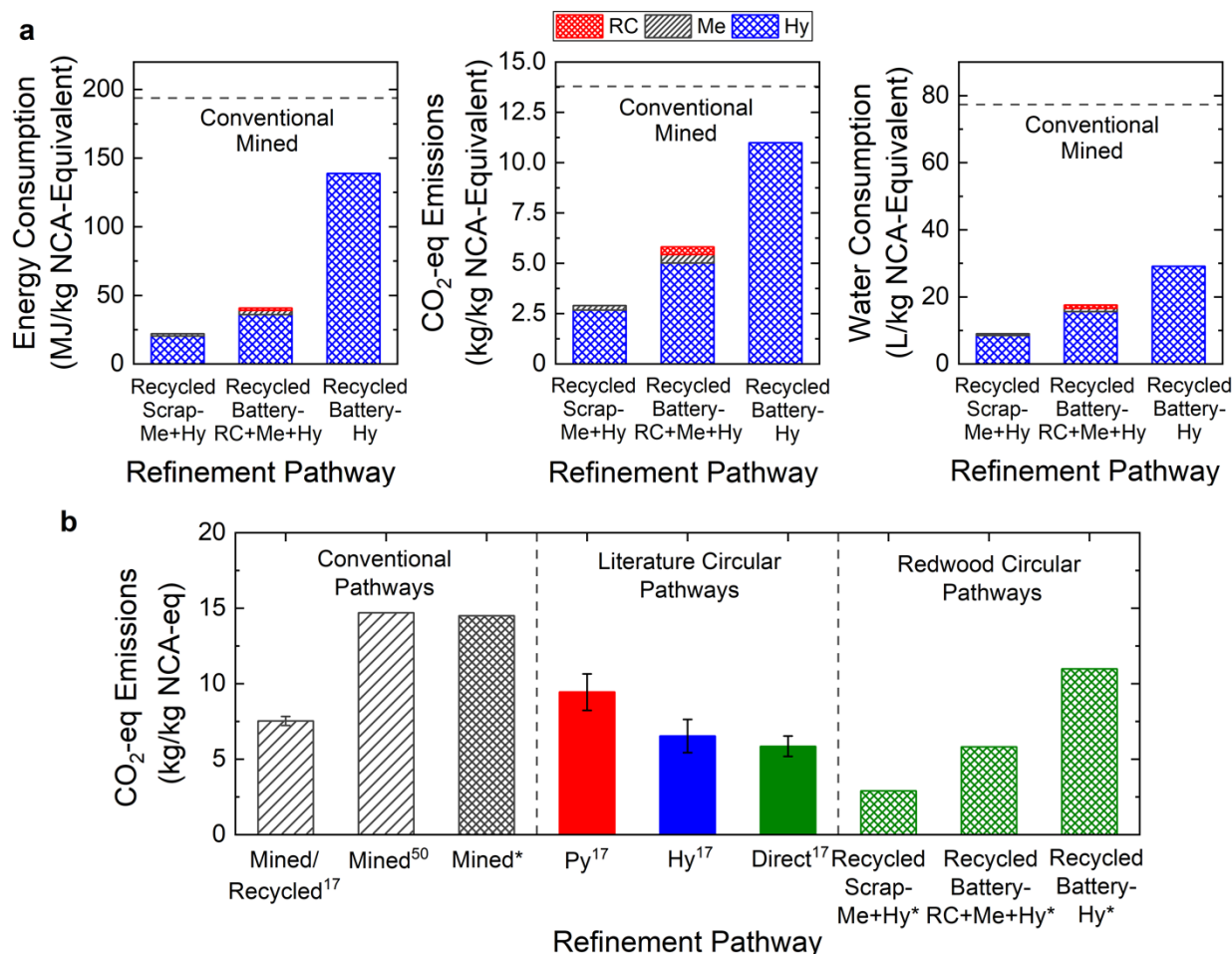
317 included because it is a common battery in consumer electronics, although it is not a common EV
 318 battery material^{48,49}.

319



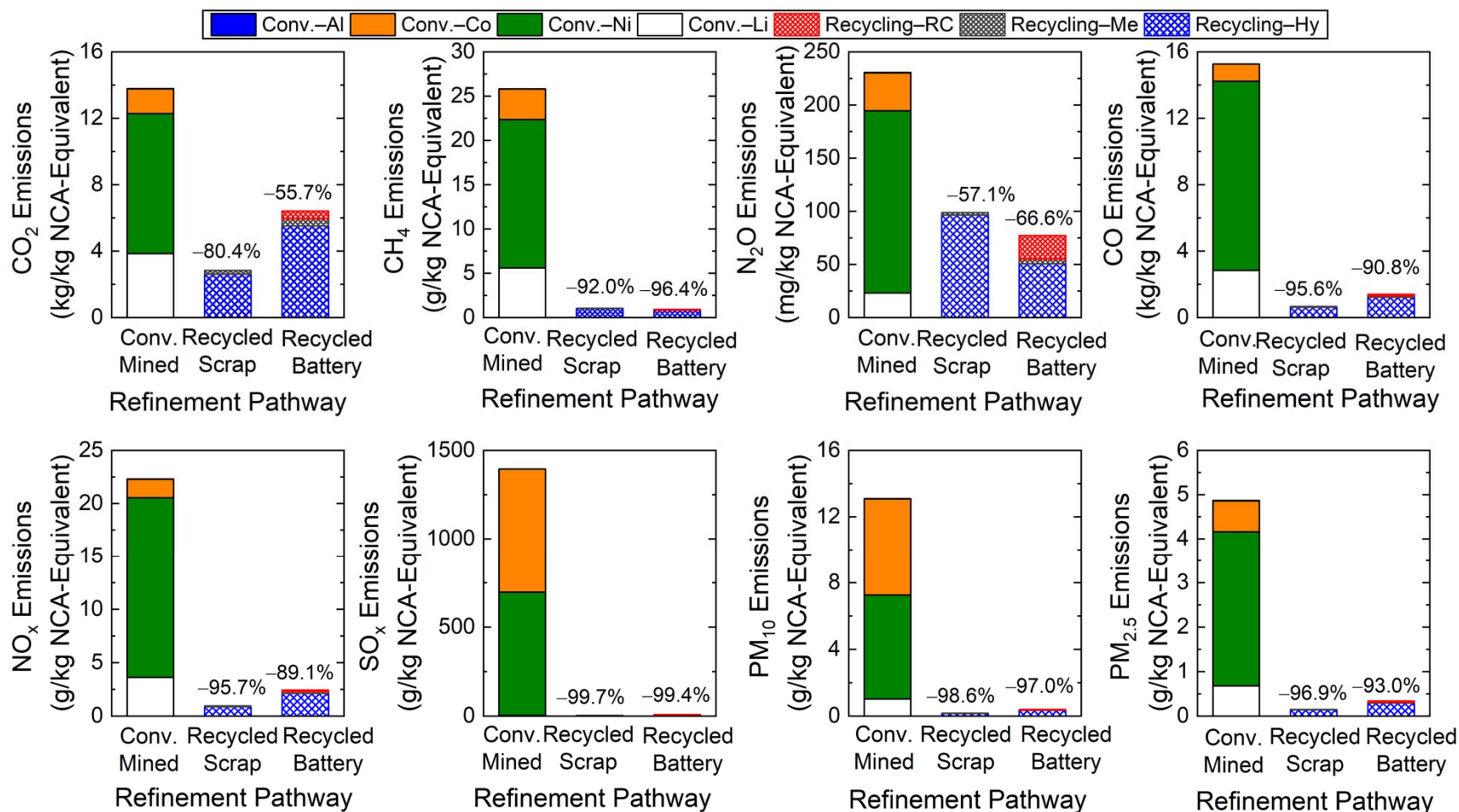
320
 321 **Fig. S2** | Gate-to-gate refinement pathways at Redwood Materials for processing two lithium-ion
 322 battery (LIB) feedstocks: LIB production scrap (recycled scrap), and LIBs collected from
 323 consumers (recycled battery). Consumables including energy, water, and chemicals are input to
 324 the refinement pathways. Three refinement processes are employed in Redwood Materials
 325 including reductive calcination (RC), mechanical processing (Me), and hydrometallurgical
 326 processing/refinement (Hy). Recycled scrap is refined by a multi-step pathway employing Me and
 327 Hy (denoted by double-line arrows), while recycled battery are refined by an RC→Me→Hy multi-
 328 step pathway (denoted by solid single arrows) and a Hy-only pathway (denoted by dashed arrows).
 329 Output products are battery-grade materials and other materials (e.g., graphite), and output
 330 emissions include greenhouse gases and SO_x, NO_x, CO, PM₁₀, and PM_{2.5}. Note that, in the system
 331 boundary, only direct processes involved in refining pathways are analyzed and no other site-wide
 332 operations (e.g., running office computers, lights) are considered.

333

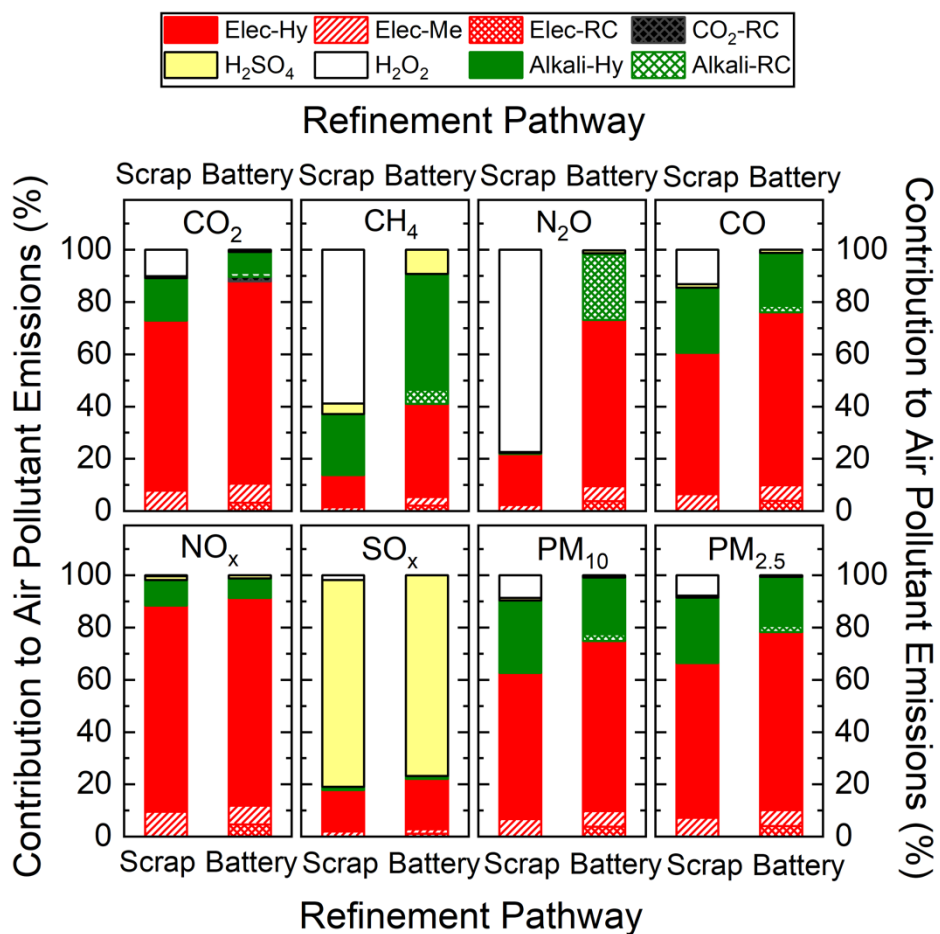


335

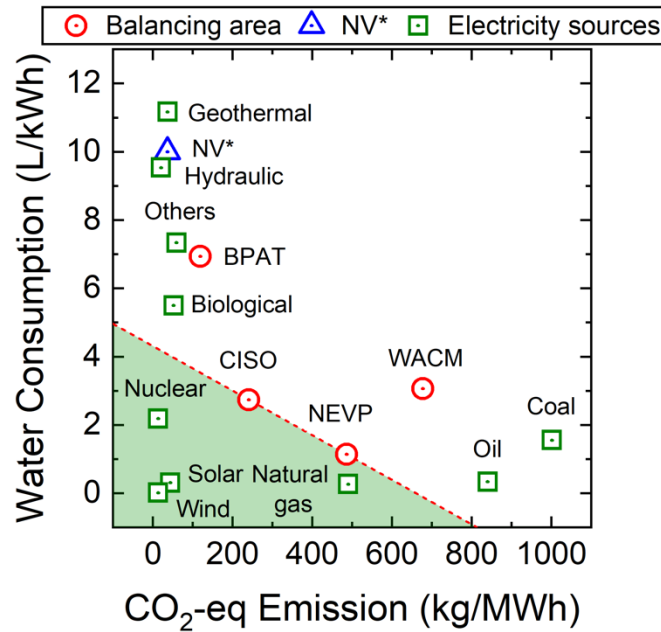
336 **Fig. S3** | a, Comparisons of the environmental metrics (i.e., energy consumption, CO₂-eq emission,
 337 and water consumption) of different refinement lithium products, Li₂SO₄ and Li₂CO₃, using
 338 Redwood (RC+Me+Hy) pathway and hydrometallurgy (Me+Hy) pathway. Both pathways refine
 339 energized batteries (recycled battery). Horizontal dash lines denote conventional mined pathways.
 340 **b**, Relative contributions of input energy, water, and consumables to the environmental metrics
 341 refining energized batteries by the hydrometallurgy (Me+Hy) pathway. **c**, Comparison of
 342 environmental impacts between refinement pathways in this study and data in literature^{17,50}. In
 343 conventional pathways, data reported in literature are based on a combined sources including
 344 mined and recycled metals, and purely mined sources. Circular pathways in literature all employ
 345 a single refinement technology, including pyrometallurgical (Py), hydrometallurgical (Hy), and
 346 direct recycling (direct). Data in this study and literature are denoted by “*” and superscripts of
 347 reference numbers, respectively. Data from the literature is normalized by the same functional unit
 348 in this study, and uncertainties are determined by combining two different battery form factors:
 349 pouch and cylindrical (detailed in **Table S14–S15**).



351
 352 **Fig. S4** | Emissions of air pollutants, including CO₂, CH₄, N₂O, CO, NO_x, SO_x, PM₁₀, and PM_{2.5}, by the mined conventional refinement
 353 and recycling processes from the scrap and energized batteries using Nevada energy (NEVP). Note that CO₂-eq emission presented in
 354 Fig. 2 is calculated by summing the greenhouse gases multiplied by the corresponding 100-year global warming potential (GWP),
 355 including CO₂ (GWP = 1), CH₄ (GWP = 25), and N₂O (GWP = 298)¹⁷.

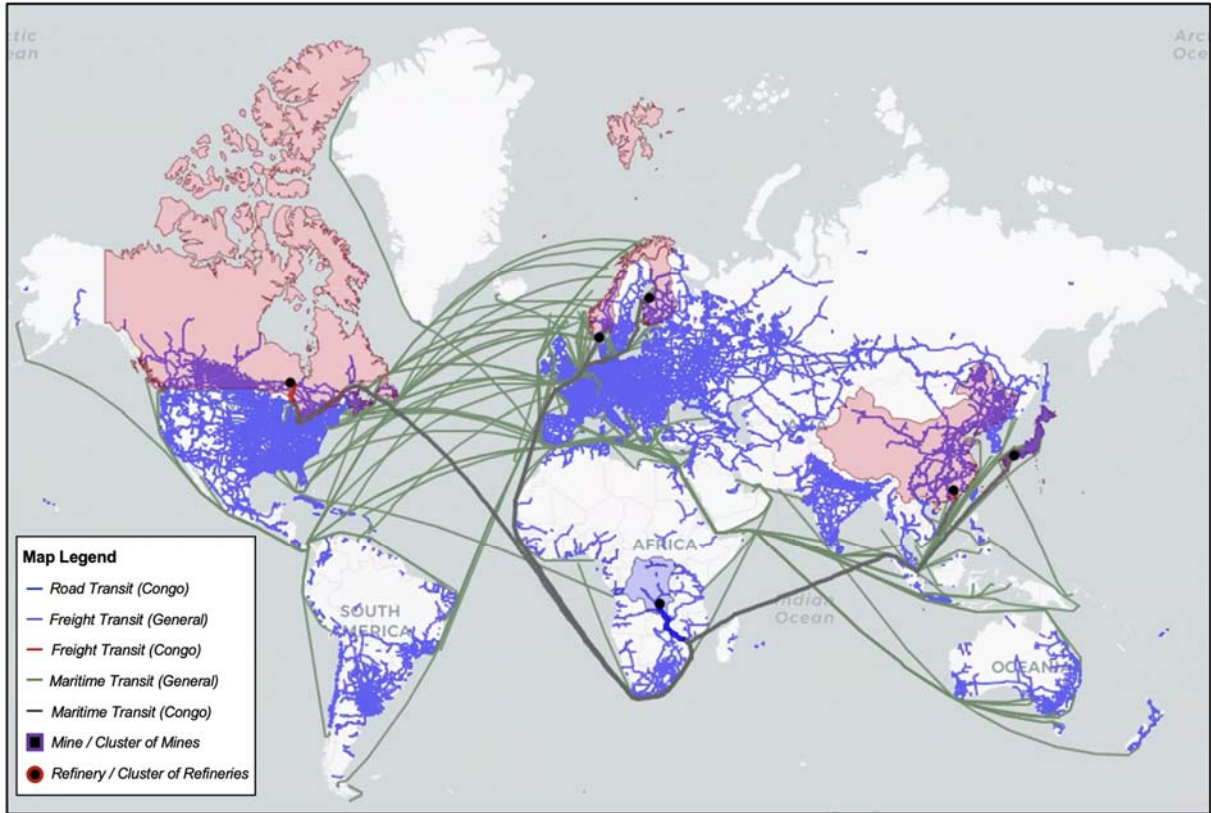


356
 357 **Fig. S5** | Relative contributions to air pollutant emissions, including CO₂, CH₄, N₂O, CO, NO_x,
 358 SO_x, PM₁₀, and PM_{2.5}, by lithium-ion battery circular refinement processes from production scraps
 359 and energized batteries based on Nevada electricity (NEVP). Note that CO₂-eq emissions
 360 presented in Fig. 2 are calculated by summing the greenhouse gases multiplied by the
 361 corresponding 100-year global warming potential (GWP), including CO₂ (GWP = 1), CH₄ (GWP
 362 = 25), and N₂O (GWP = 298)¹⁷.
 363



365
 366
 367
 368
 369
 370
 371
 372
 373
 374

Fig. S6 | Tradeoff relationship between embodied water consumption and CO₂-eq emission by different power sources, including electricity grids in different locations (⊙), purely power sources (□), and Nevada renewable energy tariff (NV*, △). The red dashed line denotes the lower bound of the water-CO₂ performance, i.e., the existing electricity grids that have the lowest water consumption and CO₂-eq emission simultaneously, and the green shaded area covers the power sources that can transcend the current limit of water-CO₂ performance. Electricity grids, including Bonneville Power Administration (BPAT), California Independent System Operator (CISO), Nevada Power Company (NEVP), and Western Area Power Administration–Colorado–Missouri (WACM), are combinations of different power sources.



375
 376
 377
 378
 379

Fig. S7 | A portion of the network model used for transportation logistics showing major road, rail, and maritime routes. The overlapping transport of cobalt concentrate from the Democratic Republic of the Congo to major global refineries is also shown^{23,24,51,52}.

380 References

- 381
- 382 1 Xu, C. *et al.* Future material demand for automotive lithium-based batteries.
383 *Communications Materials* **1**, 1-10 (2020).
- 384 2 Liu, B. *et al.* The impacts of critical metal shortage on China's electric vehicle industry
385 development and countermeasure policies. *Energy* **248**, 123646 (2022).
- 386 3 Alves Dias, P., Blagoeva, D., Pavel, C. & Arvanitidis, N. Cobalt: demand-supply balances
387 in the transition to electric mobility. *Publications Office of the European Union* **10**, 97710
388 (2018).
- 389 4 Fraser, J. *et al.* Study on future demand and supply security of nickel for electric vehicle
390 batteries. *Publication Office of the European Union: Luxembourg* (2021).
- 391 5 Valenta, R. K., Kemp, D., Owen, J. R., Corder, G. D. & Lèbre, É. Re-thinking complex
392 orebodies: Consequences for the future world supply of copper. *Journal of Cleaner*
393 *Production* **220**, 816-826 (2019).
- 394 6 Lombrana, L. M. F., J. A million tons of copper is on the way: it may not be enough. (2019).
- 395 7 Underwood, R. *et al.* Abundant Material Consumption Based on a Learning Curve for
396 Photovoltaic toward Net - Zero Emissions by 2050. *Solar RRL*, 2200705 (2022).
- 397 8 Limited, R. M. (2022).
- 398 9 Economics, T. (2022).
- 399 10 Wang, M. The greenhouse gases, regulated emissions, and energy use in transportation
400 (GREET) 2021. *Center for Transportation Research, Argonne National Laboratory* (2021).
- 401 11 Gonçalves, M. C. A. *et al.* Chemical recycling of cell phone Li-ion batteries: application
402 in environmental remediation. *Waste Management* **40**, 144-150 (2015).
- 403 12 de Chalendar, J. A., Taggart, J. & Benson, S. M. Tracking emissions in the US electricity
404 system. *Proc. Natl. Acad. Sci. U.S.A.* **116**, 25497-25502 (2019).
- 405 13 de Chalendar, J. A. & Benson, S. M. A physics-informed data reconciliation framework
406 for real-time electricity and emissions tracking. *Appl. Energy* **304**, 117761 (2021).
- 407 14 Nicholson, S. & Heath, G. Life Cycle Emissions Factors for Electricity Generation
408 Technologies. (National Renewable Energy Laboratory-Data (NREL-DATA), Golden, CO
409 (United ..., 2021).
- 410 15 Grubert, E. & Sanders, K. T. Water use in the United States energy system: a national
411 assessment and unit process inventory of water consumption and withdrawals. *Environ.*
412 *Sci. Technol.* **52**, 6695-6703 (2018).
- 413 16 Ou, L. & Cai, H. Update of Emission Factors of Greenhouse Gases and Criteria Air
414 Pollutants, and Generation Efficiencies of the US Electricity Generation Sector. (Argonne
415 National Lab.(ANL), Argonne, IL (United States), 2020).
- 416 17 Ciez, R. E. & Whitacre, J. F. Examining different recycling processes for lithium-ion
417 batteries. *Nature Sustainability* **2**, 148-156 (2019).
- 418 18 CalRecycle. *Where to recycle: Map of public recycling locations*,
419 <<https://www2.calrecycle.ca.gov/wheretorecycle/>> (2022).
- 420 19 United States Census Bureau, U. D. o. C. (2022).
- 421 20 Commission, C. E. *Zero Emission Vehicle and Infrastructure Statistics*,
422 <[https://www.energy.ca.gov/data-reports/energy-almanac/zero-emission-vehicle-and-](https://www.energy.ca.gov/data-reports/energy-almanac/zero-emission-vehicle-and-infrastructure-statistics)
423 [infrastructure-statistics](https://www.energy.ca.gov/data-reports/energy-almanac/zero-emission-vehicle-and-infrastructure-statistics)> (
- 424 21 Center for International Earth Science Information, N. Global Roads Open Access Data
425 Set (gROADS), v1 (1980–2010). *NASA Socioecon. Data Appl. Cent* (2010).

426 22 Exchange, T. H. D. (The Humanitarian Data Exchange, 2017).
427 23 Data.gov. (ed Data.gov) (2021).
428 24 Aquaplot. Aquaplot. (2021).
429 25 Maiotti, L. & Katz, B. (OECD, 2019).
430 26 Le Petit, Y. in *Transport and Environment* (2019).
431 27 Broumi, S., Bakal, A., Talea, M., Smarandache, F. & Vladareanu, L. 412-416 (IEEE).
432 28 Lopez Iii, C. E. Optimizing Energy Power Consumption of Freight Railroad Bearings
433 Using Experimental Data. (2020).
434 29 Agency, E. P. Vol. 78 FR 71903 (Environmental Protection Agency, 2014).
435 30 Kelly, J., Dai, Q., Winjobi, O. Lithium pathway updates and additions in the GREET ®
436 model. (Argonne National Laboratory, 2020).
437 31 Roithner, C., Cencic, O. & Rechberger, H. Product design and recyclability: How statistical
438 entropy can form a bridge between these concepts-A case study of a smartphone. *Journal*
439 *of Cleaner Production* **331**, 129971 (2022).
440 32 Survey, U. S. G. *Mineral commodity summaries, 2021*. (Government Printing Office,
441 2021).
442 33 Comer, B. Transitioning away from heavy fuel oil in Arctic shipping. *International Council*
443 *on Clean Transportation working paper* **3** (2019).
444 34 (ed U.S. Environmental Protection Agency) (2022).
445 35 Baumel, P., Hurburgh, C. R. & Lee, T. Estimates of total fuel consumption in transporting
446 grain from Iowa to major grain countries by alternatives modes and routes. *Iowa Grain*
447 *Quality Initiative*. Iowa (2015).
448 36 Yacobucci, B. D. & Bamberger, R. (LIBRARY OF CONGRESS WASHINGTON DC
449 CONGRESSIONAL RESEARCH SERVICE).
450 37 Davis, S. C. & Boundy, R. G. Transportation energy data book: Edition 39. (Oak Ridge
451 National Lab.(ORNL), Oak Ridge, TN (United States), 2021).
452 38 USGS. Lithium statistics and information. (U.S. Geological Surveys, 2022).
453 39 USGS. Cobalt statistics and information. (2022).
454 40 USGS. Nickel statistics and information. (U.S. Geological Surveys, 2022).
455 41 USGS. Aluminum statistics and information. (U.S. Geological Surveys, 2022).
456 42 (2022).
457 43 Li, D. Electric Vehicles to Drive Massive Battery Demand: BNEF Chart. *Bloomberg Law*
458 (2021).
459 44 Cozzi, L. *et al.* World Energy Outlook 2020. *vol* **2050**, 1-461 (2020).
460 45 Database, T. E. V. W. S. (2022).
461 46 Pillot, C.
462 47 in *Wood Mackenzie* (2020).
463 48 Chen, X., Shen, W., Vo, T. T., Cao, Z. & Kapoor, A. 230-235 (IEEE).
464 49 Zubi, G., Dufo-López, R., Carvalho, M. & Pasaoglu, G. The lithium-ion battery: State of
465 the art and future perspectives. *Renewable and Sustainable Energy Reviews* **89**, 292-308
466 (2018).
467 50 Crenna, E., Gauch, M., Widmer, R., Wäger, P. & Hischer, R. Towards more flexibility
468 and transparency in life cycle inventories for Lithium-ion batteries. *Resources,*
469 *Conservation and Recycling* **170**, 105619 (2021).
470 51 .
471 52 .
472